Quantitative structure–activity relationships (QSARs) for the transformation of organic micropollutants during oxidative water treatment

Yunho Lee [a,b], Urs von Gunten [a,c,d,*]

[a] Eawag, Swiss Federal Institute of Aquatic Science and Technology, Ueberlandstrasse 133, CH-8600 Duebendorf, Switzerland
[b] Department of Environmental Science and Engineering, Gwangju Institute of Science and Technology (GIST), Gwangju 500-712, Republic of Korea
[c] Institute of Biogeochemistry and Pollutant Dynamics, ETH Zurich, CH-8092 Zurich, Switzerland
[d] School of Architecture, Civil and Environmental Engineering (ENAC), Ecole Polytechnique Fédérale de Lausanne (EPFL), CH-1015, Lausanne, Switzerland

ARTICLE INFO

ABSTRACT

Various oxidants such as chlorine, chlorine dioxide, ferrate[VI], ozone, and hydroxyl radicals can be applied for eliminating organic micropollutant by oxidative transformation during water treatment in systems such as drinking water, wastewater, and water reuse. Over the last decades, many second-order rate constants (k) have been determined for the reaction of these oxidants with model compounds and micropollutants. Good correlations (quantitative structure–activity relationships or QSARs) are often found between the k-values for an oxidation reaction of closely related compounds (i.e. having a common organic functional group) and substituent descriptor variables such as Hammett or Taft sigma constants. In this study, we developed QSARs for the oxidation of organic and some inorganic compounds and organic micropollutants transformation during oxidative water treatment. A number of 18 QSARs were developed based on overall 412 k-values for the reaction of chlorine, chlorine dioxide, ferrate, and ozone with organic compounds containing electron-rich moieties such as phenols, anilines, olefins, and amines. On average, 303 out of 412 (74%) k-values were predicted by these QSARs within a factor of 1/3–3 compared to the measured values. For HO$^\bullet$ reactions, some principles and estimation methods of k-values (e.g. the Group Contribution Method) are discussed. The developed QSARs and the Group Contribution Method could be used to predict the k-values for various emerging organic micropollutants. As a demonstration, 39 out of 45 (87%) predicted k-values were found within a factor 1/3–3 compared to the measured values for the selected emerging micropollutants. Finally, it is discussed how the uncertainty in the predicted k-values using the QSARs affects the accuracy of prediction for micropollutant elimination during oxidative water treatment.

© 2012 Elsevier Ltd. All rights reserved.

Contents

1.   Introduction

Oxidation processes are widely applied to water treatment for the purpose of disinfection and oxidation. Target chemical pollutants for oxidation processes in drinking waters typically include inorganic (iron, manganese and arsenic, etc) and organic compounds (taste and odor compounds, fuel additives, pesticides, chlorinated solvents and algal toxins, etc). In recent years, oxidation processes have received increased attention as potential tools to eliminate so-called emerging micropollutants, such as hormones, pharmaceuticals and personal care products from wastewaters (Schwarzenbach et al., 2006, 2010; Ternes and Joss, 2006). These organic micropollutants are mainly derived from municipal wastewater effluents. Therefore, a polishing treatment of wastewater effluents by oxidation processes has been discussed and investigated from laboratory- to full-scale to minimize a discharge of micropollutants to the receiving waters (Snyder et al., 2006; Hollender et al., 2009; Gerrity et al., 2011; Zimmermann et al., 2011). Furthermore, wastewater reclamation facilities often employ multi-barrier treatment chains, which may include oxidation processes (Asano et al., 2007; Reungoat et al., 2010).

Ozone (O₃) and hydroxyl radicals (HO•) with the latter being the main oxidant in 'advanced oxidation processes (AOPs)' have gained attention as a tool to transform micropollutants during treatment of not only drinking waters but also wastewaters (von Gunten, 2003; Snyder et al., 2006). Even though chlorine dioxide (ClO₂) and chlorine (HOCl) have been used for disinfection as their primary purpose (Black & Veatch Corporation, 2010), it has been realized that certain types of organic micropollutants can be significantly transformed by ClO₂ and HOCl (Dodd and Huang, 2004, Pinkston and Sedlak, 2004; Huber et al., 2005; Deborde and von Gunten, 2008; Lee and von Gunten, 2009; Dodd et al., 2005). Additionally, ferrate^{VI} (HFeO$_4^-$) has received attention as a dual

function water treatment chemical, which can achieve oxidative transformation of micropollutants and removal of phosphate by iron-precipitation during wastewater treatment (Lee et al., 2009).

The transformation efficiency of micropollutants during oxidative water treatment depends on (1) the reactivity of the oxidant toward a target micropollutant and (2) toward the matrix components of water such as dissolved organic matter (Lee and von Gunten, 2010). The reactivity of an oxidant toward a compound has been quantified based on chemical kinetics, which employs rate laws and rate constants. Almost all reactions of water treatment oxidants (Ox) with dissolved compounds (P) typically follow second-order reaction kinetics. This yields the following rate equation:

$$P + \eta Ox \rightarrow P_{oxid} \tag{1}$$

$$-d[P]/dt = k[P][Ox] = \eta k'[P][Ox] \tag{2}$$

where k is a second-order rate constant for the consumption of P by Ox, and η is a stoichiometric factor for the amount of Ox that is depleted per P that is transformed (i.e. $k = \eta\,k'$). An integration of eq. (2) over a reaction time for a system which is closed for P (e.g. batch or plug-flow reactors) and under the condition of [P] < [Ox] yields eq. (3). The condition of [P] < [Ox] is almost always valid in oxidative water treatment because concentrations of P are in the $ng\,L^{-1}$ to $\mu g\,L^{-1}$ range while concentrations of Ox are in the $mg\,L^{-1}$ range. eq. (3) is useful when assessing and predicting micropollutant transformations during oxidative water treatment.

$$[P]_t/[P]_0 = \exp\left(-k\int_0^t [Ox]dt\right) \tag{3}$$

The k-values represent the reactivity between P and Ox quantitatively and are one of the key parameters in the kinetic

concept. Over the last decades, many k-values have been measured for the reaction of the aforementioned oxidants with a wide range of organic compounds in several different disciplines, such as water treatment chemistry, atmospheric chemistry, and biological chemistry (Buxton et al., 1988; Deborde and von Gunten, 2008; Hoigné and Bader, 1994; Lee et al., 2009; Neta et al., 1988; see also the kinetic data base Radiation Chemistry Data Center of the Notre Dame Radiation Laboratroy, available at http://kinetics.nist.gov/solution/). These k-values show that O_3, ClO_2, $HOCl$ and $HFeO_4^-$ react fast with only electron-rich organic moieties (ERMs), such as activated aromatic compounds (i.e. phenol, aniline, and polycyclic aromatics), organosulfur compounds, and deprotonated amines. Additionally, O_3 and $HFeO_4^-$ react with olefins (Lee and von Gunten, 2010). In contrast, $HO^\bullet$ react very fast with almost any type of organic moieties even including aliphatic $C-H$ bonds (Buxton et al., 1988). Based on this difference in the reactivity, O_3, ClO_2, $HOCl$ and $HFeO_4^-$ will be referred as 'selective oxidants' in the current paper as opposed to the less selective $HO^\bullet$.

Good correlations have been found between the k-values for an oxidation reaction of closely related compounds (e.g. possessing a common ERM) and substituent descriptor variables such as Hammett or Taft sigma constants (Canonica and Tratnyek, 2003). These QSARs (quantitative structure activity relationships) are useful in predicting k-values and thus transformation efficiency of micropollutants during oxidative water treatment. Especially, when considering the immense number and large structural diversity of synthetic organic compounds, which are often found in various water resources, the QSAR-based prediction method is very useful as a screening tool.

In this paper, we develop and summarize QSARs for the kinetics of the oxidation of organic compounds by the four water treatment oxidants, O_3, ClO_2, $HOCl$ and $HFeO_4^-$ (these chemical formulae indicate the actual reactive species of these oxidants under typical conditions for water treatment and will be used to refer to these oxidants) that are relevant for organic micropollutants transformation during oxidative water treatment. Existing QSARs available for the selective oxidants in literature (Canonica and Tratnyek, 2003; Deborde and von Gunten, 2008; Gallard and von Gunten, 2002; Hoigné and Bader, 1983a; Lee et al., 2005; Pierpoint et al., 2001; Rebenne et al., 1996; Suarez et al., 2007) were updated by including the latest k-values available. In addition, several new QSARs were developed in this study. For $HO^\bullet$ reactions, some principles and estimation methods of k-values are discussed. Furthermore, it was demonstrated how to use the developed QSARs to predict unknown k-values of selected organic micropollutants. Finally, the reliability and potential uncertainty involved in predicting k-values and micropollutant elimination by the QSARs are discussed.

2. Materials and methods

2.1. Source of k-values

k-Values were obtained from various literature sources: O_3 (Deborde et al., 2005; Dodd et al., 2006; Dowideit and von

Sonntag, 1998; Hoigné and Bader, 1983a,b; Neta et al., 1988; Pierpoint et al., 2001), ClO_2 (Hoigné and Bader, 1994; Huber et al., 2005; Neta et al., 1988), $HOCl$ (Deborde and von Gunten, 2008; Lee and von Gunten, 2009), and $HFeO_4^-$ (Lee et al., 2005, 2009). Some k-values of O_3 and ClO_2 are also available in an online data base, http://kinetics.nist.gov/solution/. A complete list of the references is provided in the Supporting Information, SI-Excel-1

All k-values used in the QSAR analysis correspond to species-specific reactions. Among the oxidants, only chlorine and ferrate exist in two different species under near-neutral pH conditions: $HFeO_4^- = FeO_4^{2-} + H^+$, $pK_a = 7.2$ (Sharma et al., 2001) and $HOCl = OCl^- + H^+$, $pK_a = 7.5$ (Albert and Serjeant, 1984). Since only the protonated species of chlorine and ferrate show appreciable reactivity, all k-values for chlorine and ferrate reactions correspond to the reactions of $HOCl$ and $HFeO_4^-$, respectively. Similarly among the ERMs, phenols and amines undergo acid-base speciation. In these cases, the k-values for the reaction with non-dissociated (i.e. protonated) and dissociated (i.e. deprotonated) species were treated separately.

2.2. Descriptor variables

In this study, Hammett σ (σ, σ^+ and σ^-) and Taft σ^* constants are mainly used in the QSAR analysis because they are the most common substituent descriptors in physical organic chemistry and relatively easily accessible and applicable (Hansch et al., 1991, 1995; Perrin et al., 1981). These constants are empirical parameters and obtained from thermodynamic or kinetic parameters for a specified reference reaction (e.g. ionization constants of benzoic acids) and a series of homologous reactants. These sigma constants express quantitatively the electron-donating (large negative value) or withdrawing (large positive value) properties of substituents. Hammett σ constants are typically derived from and applied to aromatic compounds and thus include inductive and resonance effects of substituents. The σ^+ and σ^- are specialized scales of σ constants, which have been used to account for the stabilization of reaction centers by resonance interaction with substituents. Therefore, the σ^+ scale differs from the σ scale for the electron-donating substituents such as alkyl-, alkoxy-, and hydroxyl-groups. In contrast, the σ^- scale differs from the σ scale for the electron-withdrawing substituents such as nitro-, acetyl-, and cyano-groups. Taft σ^* constants are derived from aliphatic compounds (e.g. ionization constants of esters) and typically represent inductive effects of substituents. Thus, Taft σ^* constants are widely used to account for substituent effects especially in aliphatic systems.

To develop QSARs for aromatic compounds (i.e. phenols, anilines, and substituted benzenes), the three σ constants (i.e. σ, σ^+, and σ^-) were tested to find the best correlations for the reaction of each selective oxidant. To account for the effects of multi-substituents on the aromatic ring, the $\sum \sigma_{o,m,p}$ (or $\sum \sigma_{o,m,p}^+$ and $\sum \sigma_{o,m,p}^-$) was used. The values were obtained by summing σ_o, σ_m, and σ_p values for each relevant substituent, which are located in *ortho*-, *meta*-, and *para*-position, respectively. Most of these constants were obtained from literature (Hansch et al., 1991, 1995). The σ_o^+ values were calculated from

the relationship $\sigma_o^+ = 0.66\sigma_p^+$, which accounts for the ortho effects (Jonsson et al., 1993). In addition, σ_o^- values were sometimes obtained from the relationship $\sigma_o^- = \sigma_p^-$ when they are not available in literature (Hansch et al., 1991, 1995).

For aliphatic compounds such as amines and olefins, Taft σ^* constants were used. The effects of substituents were accounted by using the $\sum\sigma^*$ which sums the σ^* value of each substituent around the reaction center. Amines and amine derivatives have typically three substituents on the central nitrogen atom (i.e. $R_1-N(R_2)-R_3$), thus $\sum\sigma^* = \sigma^*(R_1) + \sigma^*(R_2) + \sigma^*(R_3)$. Likewise, olefins have four substituents on the double bond (i.e. $R_1R_2-C=C-R_3R_4$), accordingly, $\sum\sigma^* = \sigma^*(R_1) + \sigma^*(R_2) + \sigma^*(R_3) + \sigma^*(R_4)$.

Descriptor variables for structurally complex substituents (especially the cases for many pharmaceuticals) were not directly available in literature. In these cases, a structural approximation has to be applied to estimate descriptor variables. The structural approximation is based on the principle that the inductive/resonance effects of atoms in substituents are attenuated with increasing distance of the atoms from a reaction center (Perrin et al., 1981). Therefore, only one or two neighboring atoms from a reaction center determine the inductive/resonance effects of whole substituents. For example, the cyclic-aliphatic ring attached to the phenolic moiety of 17α-ethinylestradiol can be approximated to *meta*- and *para*-dimethyl substituents (i.e. 3,4-dimethylphenol) because the rest of the aliphatic hydrocarbons in the rings do not have a significant influence to the electronic state of the phenolic moiety. Likewise, the structure of carbamazepine was approximated to 1,2-diphenylethene (see Supporting Information, SI-Excel-3 for more cases of structural approximations).

2.3. Linear correlations

Linear correlation equations were developed by plotting the logarithm of. k-values for reactions of oxidants with compounds versus the aforementioned substituent descriptor variables and then fitting according to the relationship, $\log(k) = \rho(\text{descriptor variable}) + y_0$, where ρ and y_0 represent the slope and intercept of the linear correlation, respectively. Cross-correlations were also tested between k-values for reaction with two oxidants. In these cases, the logarithm of k-values were fitted according to the relationship, $\log(k_1) = a \times \log(k_2) + b$. For each correlation, all k-values for the reaction with model compounds or micropollutants were used for developing QSARs. Thus, no k-values were used to test the reliability of the developed QSARs. This was because for the several investigated correlations, the k-values for the reaction with micropollutants comprise of a significant portion (on average 24%) of all available k-values. All statistical analyses were performed by a commercial software, Prism (Prism 5 for Windows, version 5.01, GraphPad Software, Inc., 2007). Further details of the QSAR analysis and results are provided in the Supporting Information, SI-EXCEL-1.

3. Results and discussions

The QSARs are presented for the reaction of the selective oxidants with four representative ERMs as reference compounds in the order of phenols, anilines, olefins, and amines. An additional QSAR is provided for the reaction of O_3 with substituted benzenes, in which benzene is used as a reference compound. This is followed by the cross-correlations among the k-values for O_3, ClO_2 and $HOCl$. All the developed QSARs are shown in Table 1 and SI-Excel-1.

3.1. QSARs of selective oxidants

3.1.1. Phenols
The four selective oxidants (O_3, ClO_2, $HOCl$ and $HFeO_4^-$) show a significant reactivity toward phenols in aqueous solution. Phenols exist as non-dissociated (PhOH) and dissociated species (PhO$^-$). Dissociated phenols have a higher electron density and thus are more reactive to electrophilic agents than non-dissociated ones. Therefore, different correlations are found for the non-dissociated and dissociated phenolic species. Figs. 1—4 show the developed correlations (k vs. σ) for each selective oxidant with dissociated phenols and non-dissociated phenols.

O_3 (Fig. 1). the linear correlations of O_3 for k_{PhOH} and k_{PhO^-} are shown in Eqs. (4) and (5) in Table 1, respectively. The $\sigma_{o,m,p}^+$ scale was the best descriptor variable for both non-dissociated and dissociated phenols. A negative slope ρ is typical for electrophilic reactions (i.e. oxidation reactions) and its magnitude reflects the sensitivity of the reaction to the substituent effect. Compared to the ρ values of other oxidants (see below), O_3 rate constants are less sensitive to the substituent variation. The k_{PhO^-}-values are typically $>10^7\,\text{M}^{-1}\,\text{s}^{-1}$, and even $>10^9\,\text{M}^{-1}\,\text{s}^{-1}$ for some phenols with electron-donating substituents (e.g. $\sum\sigma_{o,m,p}^+ < 0$). The k_{PhO^-}-values are about five orders of magnitude higher than the k_{PhOH}-values. Therefore, in near-neutral and basic solutions (e.g. pH > 7), the apparent reaction rate constants at a given pH (k_{app}) is mainly determined by the dissociated phenol species (i.e. $k_{\text{app}} = \alpha k_{\text{PhOH}} + (1-a)k_{\text{PhO}^-}$, α: degree of dissociation, $\alpha = 1/(1 + K/[\text{H}^+])$, K: dissociation constant). The reactivity pK for the ozone-phenol reaction is at about 4 (pH for which $\alpha k_{\text{PhOH}} = (1-\alpha)k_{\text{PhO}^-}$). This means that for a pH >4, ozone reacts mainly with the phenolate species. In this respect, the uncertainty of predicted k_{app}-values is mainly affected by the uncertainty of eq. (5) rather than that of eq. (4) in Table 1. 20 out of 24 (83%) k_{PhOH}-values were predicted by eq. (4) within a factor of 1/3—3 compared to the measured ones. All k_{PhO^-}-values were predicted by eq. (5) within a factor of 1/3—3. The two dotted lines around the solid line in Fig. 1 represent the prediction error range of a factor of 1/3 and 3, respectively. A prediction error range of a factor of 9 was taken in this study as practical criterion for assessing goodness of correlations. This is based on the fact that many experimentally determined rate constants even for the same reaction typically show differences of up to a factor of 10. It will be discussed later how significant the magnitude of the difference in k-value is for the uncertainty of the prediction of micropollutant elimination.

Currently, the rate constants (k_{PhOH} and k_{PhO^-}) for the reaction of O_3 are known for seven phenolic micropollutants, namely, 17α-ethinylestradiol, 17β-estradiol, estrone, estriol, bisphenol-A, 4-n-nonylphenol, and triclosan. Bisphenol-A has two pK_a values and the corresponding rate constant of the

Table 1 – Summary of the QSARs established for the selective oxidants (O_3, ClO_2, HOCl, and $HFeO_4^-$).

Eq. No.	Oxidant	Compound class	QSAR equation[a]	r^{2b}	Sy.x[c]	n^d
4	O_3	Non-dissociated phenols	$\log (k_{PhOH}) = 3.53\ (\pm 0.25) - 3.24\ (\pm 0.69)\ \Sigma\sigma^+{}_{o,m,p}$	0.81	0.38	24
5	O_3	Dissociated phenols	$\log (k_{PhO^-}) = 8.80\ (\pm 0.16) - 2.27\ (\pm 0.30)\ \Sigma\sigma^+{}_{o,m,p}$	0.96	0.26	13
6	ClO_2	Non-dissociated phenols	$\log (k_{PhOH}) = 0.41\ (\pm 0.50) - 4.69\ (\pm 1.13)\ \Sigma\sigma^+{}_{o,m,p}$	0.86	0.61	15
7	ClO_2	Dissociated phenols	$\log (k_{PhO^-}) = 8.03\ (\pm 0.13) - 3.24\ (\pm 0.28)\ \Sigma\sigma^-{}_{o,m,p}$	0.95	0.34	32
8	HOCl	Dissociated phenols	$\log (k_{PhO^-}) = 4.46\ (\pm 0.15) - 4.90\ (\pm 0.44)\ \Sigma\sigma^-{}_{o,m,p}$	0.94	0.45	35
9	$HFeO_4^-$	Non-dissociated phenols	$\log (k_{PhOH}) = 2.16\ (\pm 0.17) - 2.59\ (\pm 0.52)\ \Sigma\sigma^+{}_{o,m,p}$	0.93	0.23	11
10	$HFeO_4^-$	Dissociated phenols	$\log (k_{PhO^-}) = 4.36\ (\pm 0.13) - 3.83\ (\pm 0.48)\ \Sigma\sigma^+{}_{o,m,p}$	0.96	0.33	14
11	O_3	Anilines	$\log (k_{ArNH2}) = 7.15\ (\pm 0.25) - 1.54\ (\pm 0.42)\ \Sigma\sigma^-{}_{o,m,p}$	0.85	0.33	14
12	ClO_2	Anilines	$\log (k_{ArNH2}) = 5.34\ (\pm 0.67) - 2.47\ (\pm 0.94)\ \Sigma\sigma^+{}_{o,m,p}$	0.99	0.30	4
13	O_3	Benzene derivatives	$\log (k_{BZD}) = -0.04\ (\pm 0.38) - 3.35\ (\pm 0.26)\ \Sigma\sigma^+{}_{p}$	0.93	0.72	50
14	O_3	Olefins	$\log (k_{olefin}) = 6.18\ (\pm 0.13) - 0.49\ (\pm 0.03)\ \Sigma\sigma^*$	0.86	0.51	48
15	O_3	Amines and amine derivatives	$\log (k_{amine}) = 6.13\ (\pm 0.21) - 1.00\ (\pm 0.12)\ \Sigma\sigma^*$	0.86	0.61	54
16	ClO_2	Tertiary amines	$\log (k_{3°amine}) = 4.82\ (\pm 0.13) - 1.72\ (\pm 0.40)\ \Sigma\sigma^*$	0.86	0.19	16
17	ClO_2	Primary & secondary amines	$\log (k_{1°\&2°amine}) = 4.53\ (\pm 1.23) - 4.51\ (\pm 1.64)\ \Sigma\sigma^*$	0.79	0.95	12
18	HOCl	Tertiary amines	$\log (k_{3°amine}) = 4.79\ (\pm 0.29) - 1.96\ (\pm 0.80)\ \Sigma\sigma^*$	0.86	0.27	8
19	HOCl	Primary amines & amine derivatives	$\log (k_{1°amine}) = 9.70\ (\pm 0.32) - 2.10\ (\pm 0.18)\ \Sigma\sigma^*$	0.97	0.43	22
20	O_3/ClO_2	Aromatics	$\log k_{aromatic} (O_3) = 3.19\ (\pm 0.57) + 0.76\ (\pm 0.11)\ \log k_{aromatic} (ClO_2)$	0.94	0.58	16
21	$O_3/HOCl$	Aromatics	$\log k_{aromatic} (O_3) = 4.50\ (\pm 0.38) + 0.96\ (\pm 0.11)\ \log k_{aromatic} (HOCl)$	0.94	0.66	24

a In QSAR equations, values in parentheses are 95 % confidence intervals.
b r^2 is the coefficient of correlation.
c Sy.x is the standard deviation of the linear regression and calculated as Sy.x $= (SS/df)^{1/2}$ where SS is the sum-of-squares of the distance of the linear regression from the data points and df is the degrees of freedom of the fit (i.e. $n - 2$).
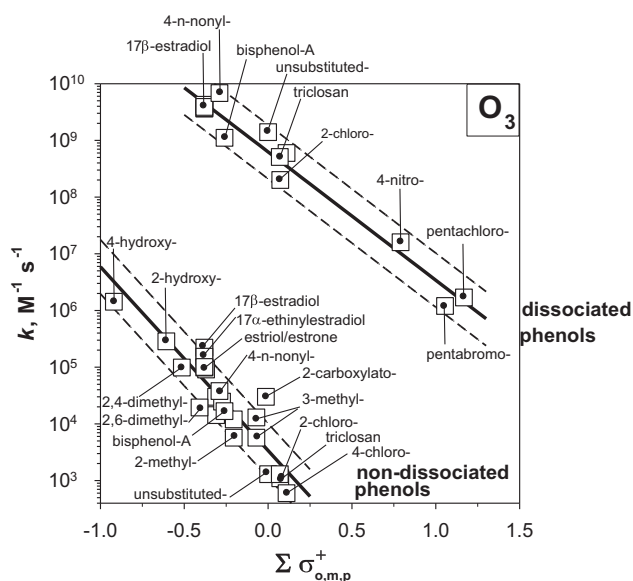d n is the number of data points.

Fig. 1 – Correlations between the second-order rate constants (k) for the reactions of ozone (O_3) with non-dissociated phenols (eq. (4), Table 1) and dissociated phenols (eq. (5), Table 1) vs. $\sum\sigma^+_{o,m,p}$. Solid lines represent the obtained linear equations and dash lines represent the prediction error ranges of a factor of 1/3 and 3, respectively. Some symbols are not named due to space limitation: dissociated phenols such as 4-chlorophenolate, 17α-ethinylestradiol, estrone and estriol, non-dissociated phenols such as 4-methyl-, 2,3-dimethyl-, 3-hydroxy- and 3,4-dimethyl-phenol. The corresponding data can be found in SI-Excel-1.
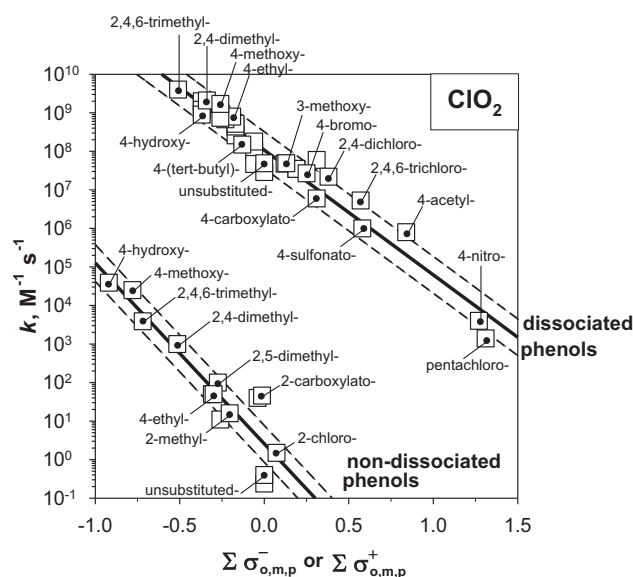
Fig. 2 – Correlations between the second-order rate constants (k) for the reactions of chlorine dioxide (ClO_2) with non-dissociated phenols vs. $\sum\sigma^+_{o,m,p}$ (eq. (6), Table 1), and with dissociated phenols vs. $\sum\sigma^-_{o,m,p}$ (eq. (7), Table 1). Some symbols are not named due to space limitation: dissociated phenols such as 2-carboxylato-, 2-chloro-, 4-chloro-, 2-hydroxy-, 3-hydroxy-, 2-methoxy-, 2-methyl-, 3-methyl-, 4-methyl-, 2,5-dimethyl-phenolate, tyrosine and 17α-ethinylestradiol: non-dissociated phenols such as 4-cyano-, 4-tert-butyl-, 3-hydroxy-, 2-methoxy-, 4-methyl-, 4-nitro-, 4-sulfonato-, tyrosine, 4-bromo-, and 4-cyanophenol (data, SI-EXCEL-1).
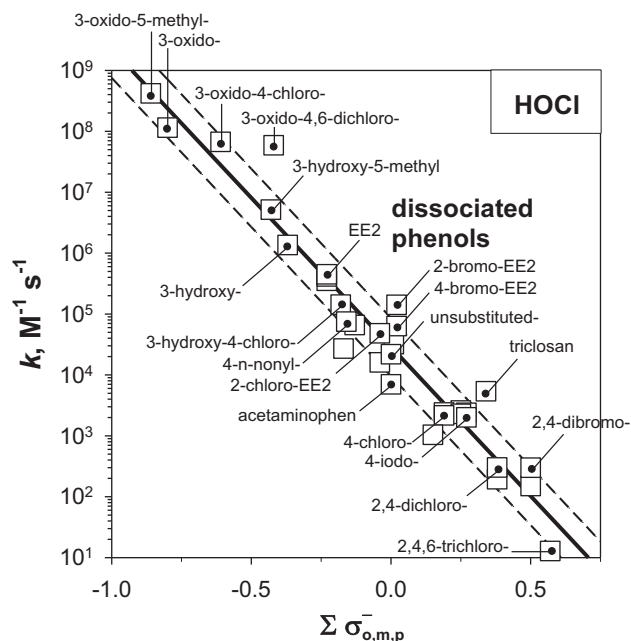
Fig. 3 – Correlation between the second-order rate constants (k) for the reactions of chlorine (HOCl) with dissociated phenols vs. $\sum \sigma_{o,m,p}^-$ (eq. (8), Table 1). EE2 represent 17α-ethinylestradiol. Some symbols are not named due to space limitation: 2-chloro-, 2,6-dichloro-, 2-bromo-, 4-bromo-, 2,6-dibromo-, 3-hydroxy-4,6-dichloro- and 4-methyl-phenol, and bisphenol-A, 17β-estradiol, estrone, estriol, 4-chloro-EE2, 2,4-dichloro-EE2 and 2,4-dibromo-EE2 (data, SI-EXCEL-1).

single-dissociated $(k_{BPA^-} = 1.06 \times 10^9 \, M^{-1} \, s^{-1})$ and doubly-dissociated species $(k_{BPA2^-} = 1.11 \times 10^9 \, M^{-1} \, s^{-1})$ are reported (Deborde et al., 2005). The two nearly identical rate constant indicate that dissociation of one phenol has little influence to
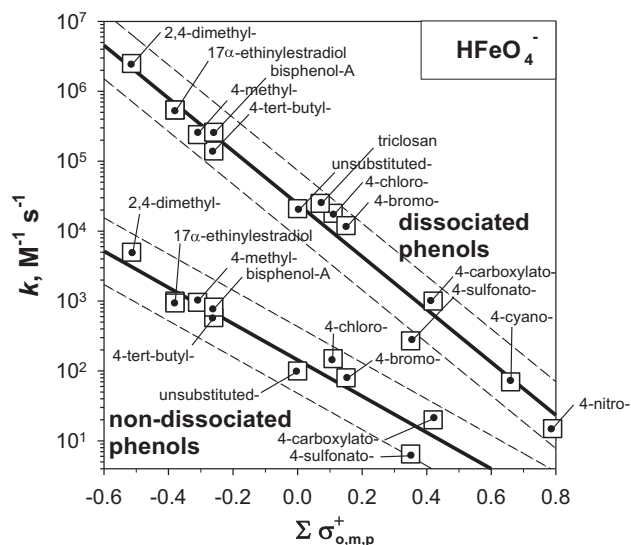

Fig. 4 – Correlation between the second-order rate constants (k) for the reactions of ferrate^{VI} (HFeO$_4^-$) with non-dissociated phenols (eq. (9), Table 1) and dissociated phenols vs. $\sum \sigma_{o,m,p}^+$ (eq. (10), Table 1) (data, SI-EXCEL-1).

the electronic state of the other phenol in bisphenol-A. In this study, the k-value of $1.1 \times 10^9 \, M^{-1} \, s^{-1}$ was therefore used for the two dissociated species of bisphenol-A. In all cases except the k_{PhOH}-value for 17α-ethinylestradiol and 17β-estradiol, the measured and predicted rate constants differ by less than a factor of 3. However, the predicted k_{PhO^-}-value for 17α-ethinylestradiol and 17β-estradiol were lower than the measured ones by a factor of 3.2 and 3.8, respectively. (see Table 2 and SI-Excel-1).
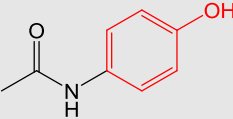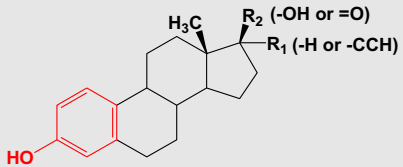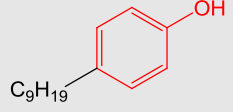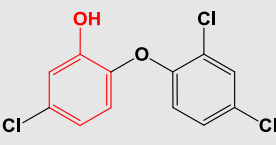
ClO_2 (Fig. 2). The linear correlations of ClO$_2$ for both k_{PhOH} and k_{PhO^-} are shown in Eqs. (6) and (7) in Table 1, respectively. The $\sigma_{o,m,p}^+$ scale was the best descriptor variables for non-dissociated phenols, while the $\sigma_{o,m,p}^-$ scale was the best for dissociated phenols (see SI-Excel-1). eq. (7) is quite similar to the QSAR equation developed by Tratnyek and Hoigne (i.e. $\log(k_{PhO^-}) = 8.2(\pm 0.2) - 3.2(\pm 0.4) \sum \sigma_{o,m,p}^-$, $n = 23$, $s = 0.39$, $r = 0.97$) (Tratnyek and Hoigne, 1994). Compared to O$_3$, ClO$_2$ shows at least one order of magnitude lower k_{PhO^-}-values. The k_{PhO^-}-values are about eight orders of magnitude higher than the k_{PhOH}-values. Therefore, the k_{app}-values are controlled by the concentration of dissociated phenols (reactivity pK is about 2), which is similar to the case of O$_3$. 10 out of 15 (67%) k_{PhOH}-values were predicted by eq. (6) within a factor of 1/3–3 compared. 25 out of 32 (78%) k_{PhO^-}-values were predicted by eq. (7) within a factor of 1/3–3. Among various phenolic micropollutants, only the k_{PhO^-}-value for 17α-ethinylestradiol is known, which was well correlated with eq. (7) (a factor of 1.3 difference) (see Table 2 and SI-Excel-1).

$HOCl$ (Fig. 3). For HOCl, the best correlation is obtained for $\sigma_{o,m,p}^-$ and shown in eq. (8) in Table 1. A very poor correlation was found for the reaction of HOCl with PhOH (e.g. $r^2 = 0.36$). The poor correlation might be due to the poor reliability of the k_{PhOH}-values. At acidic pH, the reaction of Cl$_2$ with PhOH (or acid-catalyzed reaction of HOCl, i.e. H$^+$ + HOCl + PhOH) becomes important (Deborde and von Gunten, 2008) and therefore the k_{PhOH}-values cannot be determined with accuracy because of the relative minor contribution of the reaction between HOCl and PhOH to the overall reaction.
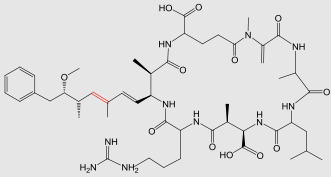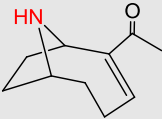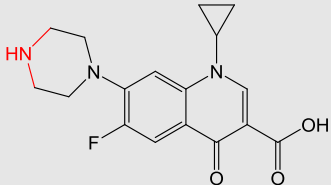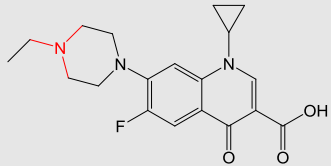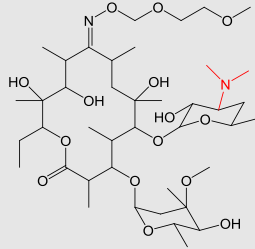
Eq. (8) includes the k_{PhO^-}-values with *meta*-hydroxyphenol, which could not be well correlated with those of other phenols by using the $\sigma_{o,m,p}^+$ or $\sigma_{o,m,p}$ scale in previous studies (Deborde and von Gunten, 2008; Gallard and von Gunten, 2002; Rebenne et al., 1996). Therefore, the $\sigma_{o,m,p}^-$ scale was investigated instead of $\sigma_{o,m,p}^+$ or $\sigma_{o,m,p}$ scale in this case. The σ_m^- value for oxido substituent (−O$^-$) was not available in literature, therefore it was estimated in this study by trial-and-error approach. The σ_m^- value for oxido substituent was initially guessed as '−0.82' from the σ_p^- value for oxido substituent. The guessed value was used to calculate $\sum \sigma_{o,m,p}^-$ values of 3-oxido-, 3-oxido-4-chloro- and 3-oxido-5-methyl-phenolates that were included in generating eq. (8). Next, a range of σ_m^- values (e.g. −0.82 ±0.3) was tested to yield a best correlation coefficient (r^2) for eq. (8). A value of '−0.8' resulted from this procedure. Based on the obtained $\sigma_{o,m,p}^-$ scale, the k_{PhO^-}-values for *meta*-hydroxyphenols could be well correlated with those of other phenols.

HOCl shows about four orders of magnitude lower k_{PhO^-}-values than O$_3$. In addition, the k_{PhO^-}-values are more sensitive to the substituent variation than any other oxidants with a ρ slope of −4.9 (even considering the difference in the σ

Table 2 — Prediction of second-order rate constants (k) by using QSARs developed for the reaction of selective oxidants (O_3, ClO_2, HOCl, and $HFeO_4^-$) and $HO^\bullet$ (Group Contribution Method, GCM) with selected micropollutants.

Micropollutant	$\sum \sigma^+_{o,m,p}$ [a]	$\sum \sigma^-_{o,m,p}$ [a]	$\sum \sigma^*$ [b]	Reaction	Measured k (M^{-1}s^{-1})[c]	Predicted k (M^{-1}s^{-1})	k_{app} at pH 7 (M^{-1}s^{-1})[d]	k_{pred}/k_{meas} [e]	Method[f]
Phenols									
	0	0	—	$HO^\bullet$	—	5.8×10^9	5.8×10^9	—	GCM[g]
				O_3 + phenol	—	3.4×10^3	1.3×10^6	—	eq. (4)
				O_3 + phenolate	—	6.3×10^8		—	eq. (5)
				ClO_2 + phenol	—	2.6		—	eq. (6)
				ClO_2 + phenolate	—	1.1×10^8	2.1×10^5	—	eq. (7)
				HOCl + phenolate	7.0×10^3	2.9×10^4	1.1×10^1	4.1	eq. (8)
				$HFeO_4^-$ + phenol	—	1.4×10^2	1.2×10^2	—	eq. (9)
Acetaminophen $pK_a = 9.7$ (analgesic)				$HFeO_4^-$ + phenolate	—	2.3×10^4		—	eq. (10)
				$HO^\bullet$	10×10^9	10×10^9	10×10^9	1.0	GCM[g]
				O_3 + phenol	—	2.4×10^4	7.2×10^5	—	eq. (4)
				O_3 + phenolate	1.1×10^9	2.4×10^9		2.2	eq. (5)
	−0.26	−0.13	—	ClO_2 + phenol	—	4.3×10^1	1.8×10^5	—	eq. (6)
				ClO_2 + phenolate	—	2.8×10^8		—	eq. (7)
				HOCl + phenolate	6.6×10^4	1.2×10^5	3.2×10^1	1.9	eq. (8)
				$HFeO_4^-$ + phenol	8.2×10^2	6.8×10^3	6.2×10^2	0.8	eq. (9)
Bisphenol-A $pK_a = 9.6$ and 10.2 (plasticizer)				$HFeO_4^-$ + phenolate	2.6×10^5	2.3×10^5		0.9	eq. (10)
				$HO^\bullet$	$(9.8-14) \times 10^9$ [h]	10×10^9	$\sim 10 \times 10^9$	≤ 1.4	GCM[g]
				O_3 + phenol	$(1.0-2.2) \times 10^5$ [h]	5.8×10^4	1.6×10^6	~ 0.3	eq. (4)
				O_3 + phenolate	$(3.7-4.2) \times 10^9$ [h]	4.6×10^9		~ 1.2	eq. (5)
	−0.38	−0.23	—	ClO_2 + phenol	—	1.6×10^2		—	eq. (6)
				ClO_2 + phenolate	4.6×10^8 [h]	6.0×10^8	1.8×10^5	1.3	eq. (7)
				HOCl + phenolate	$(3.5-4.5) \times 10^5$ [h]	3.9×10^5	1.1×10^2	1.1	eq. (8)
				$HFeO_4^-$ + phenol	$(9.4-10) \times 10^2$ [h]	1.4×10^3	7.3×10^2	1.5	eq. (9)
Steroid estrogens[h] $pK_a = \sim 10.4$				$HFeO_4^-$ + phenolate	5.4×10^5 [h]	6.5×10^5		1.2	eq. (10)
				$HO^\bullet$	—	10×10^9	10×10^9	—	GCM[g]
				O_3 + phenol	3.8×10^4	3.0×10^4	1.4×10^6	0.8	eq. (4)
				O_3 + phenolate	6.8×10^9	2.9×10^9		0.4	eq. (5)
	−0.29	−0.16	—	ClO_2 + phenol	—	5.9×10^1	7.1×10^4	—	eq. (6)
				ClO_2 + phenolate	—	3.6×10^8		—	eq. (7)
				HOCl + phenolate	7.5×10^4	1.8×10^5	1.1×10^1	2.3	eq. (8)
				$HFeO_4^-$ + phenol	—	8.1×10^3	5.5×10^2	—	eq. (9)
4-n-Nonylphenol $pK_a = 10.7$ (nonionic surfactant degradation product)				$HFeO_4^-$ + phenolate	—	2.9×10^5		—	eq. (10)
				$HO^\bullet$	—	9.7×10^9	9.7×10^9	—	GCM[g]
				O_3 + phenol	1.3×10^3	2.0×10^3	3.8×10^7	1.5	eq. (4)
				O_3 + phenolate	5.1×10^8	4.4×10^8		0.9	eq. (5)
	0.07	0.34	—	ClO_2 + phenol	—	1.2	6.3×10^5	—	eq. (6)
				ClO_2 + phenolate	—	8.5×10^6		—	eq. (7)
				HOCl + phenolate	5.4×10^3	6.2×10^2	3.0×10^2	0.1	eq. (8)
				$HFeO_4^-$ + phenol	—	9.5×10	1.2×10^3	—	eq. (9)
Triclosan $pK_a = 8.1$ (antimicrobial disinfectant)				$HFeO_4^-$ + phenolate	2.5×10^4	1.2×10^4		0.5	eq. (10)

(continued on next page)

Table 2 — (continued)

Micropollutant	$\sum \sigma^+_{o,m,p}$ [a]	$\sum \sigma^-_{o,m,p}$ [a]	$\sum \sigma^*$ [b]	Reaction	Measured k (M^{-1} s^{-1})[c]	Predicted k (M^{-1} s^{-1})	k_{app} at pH 7 (M^{-1} s^{-1})[d]	k_{pred}/k_{meas}[e]	Method[f]
Anilines									
Sulfamethoxazole (antibiotic)	0.57	0.94	—	HO$^\bullet$	5.5×10^9	$8.1 \times 10^{9*}$	5.5×10^9	1.5	GCM[g]
				O$_3$	5.7×10^5	5.0×10^5	5.7×10^5	0.9	eq. (11)
				ClO$_2$	7.9×10^3	8.5×10^3	7.9×10^3	1.1	eq. (12)
Diclofenac pK$_a$ = 4.2 (nonsteroidal anti-inflammatory)	—	—	—	HO$^\bullet$	7.5×10^9	10×10^9	7.5×10^9	1.3	GCM[g]
				O$_3$	1×10^6	1.8×10^6	1×10^6	1.8	eq. (20)
				ClO$_2$	1.1×10^4	5.1×10^3	1.1×10^4	0.5	eq. (20)
				HOCl	—	3.7×10^1	2.8×10^1	—	eq. (21)
Benzene derivatives									
Gemfibrozil (antilipidemic)	−1.4[i]	—	—	HO$^\bullet$	10×10^9	10×10^9	10×10^9	1.0	GCM[g]
				O$_3$	—	4.6×10^4	4.6×10^4	—	eq. (13)
						2.3×10^4	2.3×10^4	—	eq. (21)
				ClO$_2$	—	5.9×10^1	5.9×10^1	—	eq. (20)
				HOCl	0.7	—	0.5	—	—
Naproxen (nonsteroidal anti-inflammatory)	—	—	—	HO$^\bullet$	9.6×10^9	10×10^9	9.6×10^9	1.0	GCM[g]
				O$_3$	2.0×10^5	7.4×10^4	2.0×10^5	0.4	eq. (21)
				ClO$_2$	—	6.1×10^2	6.1×10^2	—	eq. (20)
				HOCl	2.4	6.8	1.8	2.8	eq. (21)
Olefins									
Anatoxin-protonated (cyanotoxin)	—	—	3.60	HO$^\bullet$	3×10^9	10×10^9	3×10^9	3.3	GCM[g]
				O$_3$	2.8×10^4	2.4×10^4	2.8×10^4	0.9	eq. (14)
				HFeO$_4^-$	—	6–20	3.8–13	—	—[j]
Carbamazepine (antiepileptic/analgesic)	—	—	2.48	HO$^\bullet$	8.8×10^9	10×10^9	8.8×10^9	1.1	GCM[g]
				O$_3$	3×10^5	9.4×10^4	3×10^5	0.3	eq. (14)
				HFeO$_4^-$	1.1×10^2	$(0.6–2) \times 10^2$	6.9×10^1	<2	—[j]

Microcystin-LR (cyanotoxin)

—	—	1.29			
HO•	10×10^9	10×10^9	10×10^9	1.0	GCM[g]
O3	4.1×10^5	3.5×10^5	4.1×10^5	0.8	eq. (14)
HFeO4$^-$	—	$(0.8-2.7) \times 10^2$	$(0.5-1.7) \times 10^2$	—	—[j]

Amines

Anatoxin-a-deprotonated pK$_a$ = 9.36 (cyanotoxin)

—	—	0.11			
HO•	3×10^9	10×10^9	310^9	3.3	GCM[g]
O3	8.7×10^5	1.0×10^6	3.8×10^3	1.2	eq. (14)
ClO2	—	1.1×10^4	4.7×10^1	—	eq. (17)
HOCl	—	$(1-7) \times 10^7$	$(0.3-2.3) \times 10^5$	—	—[j]

Ciprofloxacin pK$_a$ = 8.8 (antibiotic)

—	—	0.59			
HO•	4.1×10^9	10×10^9	4.1×10^9	2.4	GCM[g]
O3	9.0×10^5	3.5×10^5	1.4×10^4	0.4	eq. (15)
ClO2	—	7.8×10^1	1.2	—	eq. (17)
HOCl	4.9×10^7	$(1-7) \times 10^7$	5.8×10^5	<5	—[k]

Enrofloxacin pK$_a$ = 7.7 (antibiotic)

—	—	0.0			
HO•	4.5×10^9	10×10^9	4.5×10^9	2.2	GCM[g]
O3	7.8×10^5	1.3×10^6	1.3×10^5	1.7	eq. (15)
ClO2	—	3.5×10^4	5.9×10^3	—	eq. (17)

Roxithromycin pK$_a$ = 9.2 (antibiotic)

—	—	0.15			
HO•	5.4×10^9	$10 \times \times 10^9$	5.4×10^9	1.9	GCM[g]
O3	4.5×10^6	9.4×10^5	2.8×10^4	0.2	eq. (15)
ClO2	1.4×10^4	3.6×10^4	8.8×10^1	2.6	eq. (16)
HOCl	—	3.1×10^4	1.5×10^2	—	eq. (18)

The reactive sites of micropollutants as the electron-rich moieties (ERM) were marked in red color (Further details are given in the Supporting Information, SI-Excel-2 and SI-Excel-3).

a Hammett sigma constants calculated from Hansch et al. (1991,1995).

b Taft sigma constants calculated from Perrin et al. (1981).

c For sources of k-values, see SI-Excel-2 and SI-Excel-3.

d $k_{app} = \alpha k_{PhOH} + (1 - \alpha)k_{PhO^-}$ for phenolic compounds and $k_{app} = (1 - \alpha)k_{amine}$ for amine compounds, α: degree of dissociation, $\alpha = 1/(1 + K/[H^+])$, K: dissociation constant, and only when k_{meas} data are not available, k_{pred} are applied for calculation.

e Ratio of the predicted (k_{pred}) and measured k-values (k_{meas}).

f Methods used to predict k-values.

g Group Contribution Method (Eq. (23)).

h Measured k-value ranges are for steroid estrogens such as 17α-ethinylestradiol, 17β-estradiol, estrone, and estriol.

i $\sum \sigma_p^+$ value.

j Rough estimate based on the 500–1500-fold low reactivity of $HFeO_4^-$ than O_3 toward olefins.

k Rough estimate based on the range of the k-values for the reaction of HOCl with 2° alkylamines.

scale). The k_{PhO^-}-values are about four orders of magnitude higher than the k_{PhOH}-values, therefore the k_{app}-values are also controlled by the concentration of dissociated phenols, which is similar to the case of O_3 and ClO_2. 28 out of 35 (80%) k_{PhO^-}-values were predicted by eq. (8) within a factor of 1/3–3. Currently, the k_{PhO^-}-values for the reaction of HOCl are known for fourteen phenolic micropollutants. These include acetaminophen, bisphenol-A, 2-bromo-17α-ethinylestradiol (2-bromo EE2), 4-bromo EE2, 2-chloro EE2, 4-chloro EE2, 2,4-dibromo-EE2, 2,4-dichloro-EE2, EE2, 17β-estradiol (E2), estriol (E3), estrone (E1), 4-nonylphenol, and triclosan. In most cases, eq. 8 yields good predictions for the k_{PhO^-}-values of these micropollutants with differences of less than a factor of 3. However, the predicted k_{PhO^-}-value for acetaminophen was lower than the measured one by a factor of 4.1. In addition, the predicted k_{PhO^-}-value for triclosan was higher than the measured one by a factor of 8.6 (see Table 2 and SI-Excel-1).

$HFeO_4^-$ (Fig. 4). For $HFeO_4^-$, the best correlations are obtained when using $\sigma_{o,m,p}^+$ scales and are shown in Eqs. 9 and 10 in Table 1, respectively. The k_{PhO^-}-values of $HFeO_4^-$ were similar to HOCl but several orders of magnitude lower than those of O_3 and ClO_2. Interestingly, the k_{PhOH}-values of $HFeO_4^-$ were considerably higher than those of ClO_2 and HOCl. In addition, the k_{PhOH}-values were just about two orders of magnitude lower than the k_{PhO^-}-values, which is a relatively small difference compared to those of other oxidants (e.g. more than four orders of magnitude difference for O_3, ClO_2 and HOCl). From the comparison of the ρ slopes, $HFeO_4^-$ was found less selective to non-dissociated phenols ($\rho = -2.59$) than dissociated ones ($\rho = -3.78$), which is in contrast to the cases of O_3 and ClO_2. These observations seem to suggest that the mechanism for the reaction of $HFeO_4^-$ with non-dissociated phenols is different from that with dissociated phenols.

Due to the small difference in the k_{PhOH}- and k_{PhO^-}-values, both non-dissociated and dissociated phenol species are important in controlling the k_{app}-values. The reactivity pK for 17α-ethinylestradiol is at 7.5. Therefore, the k_{app}-values are controlled by the fraction of non-dissociated phenols at pH <7.5 while it is dominated by the fraction of dissociated phenols at pH >7.5 (see above).

All 11 k_{PhOH}-values were predicted by eq. (9) with a difference of less than a factor of 3. 13 out of 14 (93%) k_{PhO^-}-values were predicted by eq. (10) within less than a factor of 3. Currently, the rate constants (k_{PhOH} and k_{PhO^-}) for the reaction of $HFeO_4^-$ are known for four phenolic micropollutants, namely, bisphenol-A, 17α-ethinylestradiol, 17β-estradiol and triclosan. For these four micropollutants, the predicted k-values lie within a factor of 2 relative to the measurements (see Table 2 and SI-Excel-1).

3.1.2. Anilines

All selective oxidants show a high reactivity to anilines ($k > 10^2\ M^{-1}\ s^{-1}$). Compared to phenols, however, the number of available k-values is significantly lower for ClO_2, HOCl, and $HFeO_4^-$. The three sets of Hammett σ constants were tested for the correlation analysis.

O_3 (Fig. 5). The linear correlation of O_3 for k_{ArNH2} is shown in eq. (11) in Table 1. For ozone, the $\sigma_{o,m,p}^-$ scale yielded the best correlation. Even though the k_{ArNH2}-values are one or two orders of magnitude lower than k_{PhO^-}-values (eq. (5) vs. eq.
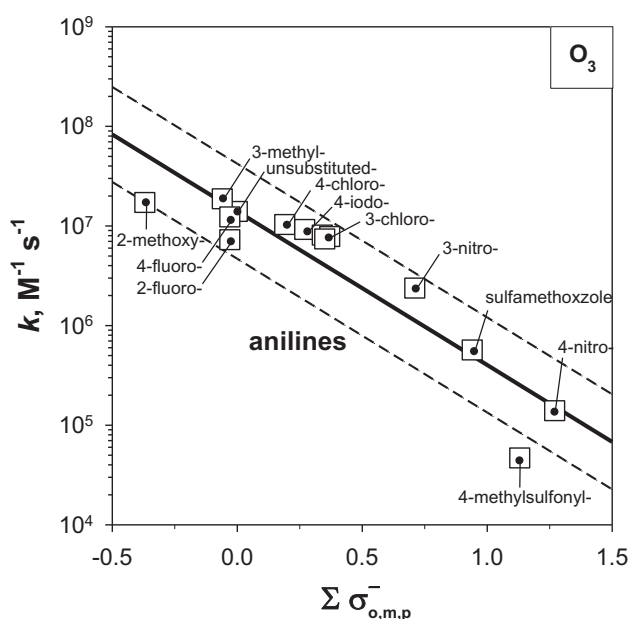
Fig. 5 – Correlation between the second-order rate constants (k) for the reactions of O_3 with anilines vs. $\sum \sigma^-_{o,m,p}$ (Eq. (11), Table 1) (data, SI-EXCEL-1).
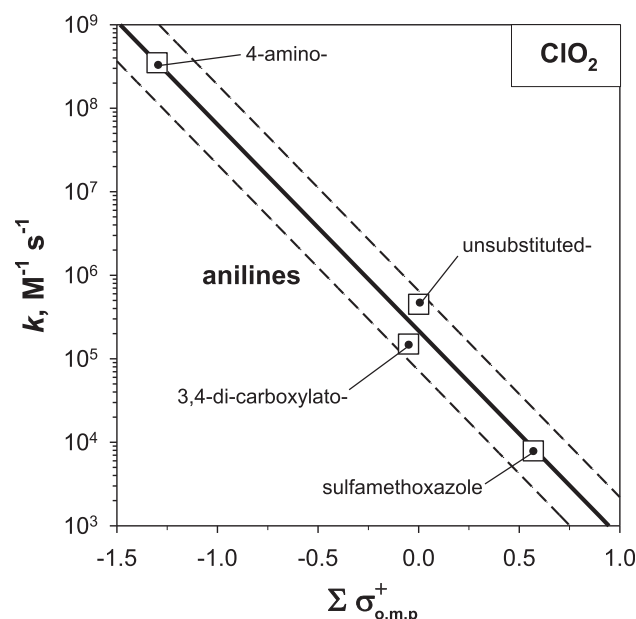

Fig. 6 – Correlation between the second-order rate constants (k) for the reactions of ClO_2 with anilines vs. $\sum \sigma^+_{o,m,p}$ (Eq. (12), Table 1) (data, SI-EXCEL-1).

(11)), the k_{app}-values for the reaction of O_3 at near-neutral pH are higher with anilines than phenols because anilines do not change their speciation (pK$_a$ values of anilines <5). The ρ slope is −1.54, thus the reactions are relatively less sensitive to the substituent effects. 12 out of 14 (86%) k_{ArNH2}-values were predicted by Eq. (11) within a factor 1/3–3. Currently, the k_{ArNH2}-value of O_3 is known only for sulfamethoxazole as aniline-containing micropollutants. Eq. (11) predicts well the k_{ArNH2}-value of sulfamethoxazole within a factor of 1.2 (see Table 2 and SI-Excel-1).

ClO_2 (Fig. 6). The linear correlation of ClO_2 for k_{ArNH2} is shown in Eq. (12) in Table 1. Compared to O_3, ClO_2 shows about two orders of magnitude lower k-values for non-substituted aniline. Because of the small number of k-values available (n = 4), the obtained correlation for ClO_2 is less reliable than other correlations presented in this study. Nevertheless, the k_{ArNH2}-value for the reaction of chlorine dioxide with sulfamethoxazole is well correlated with Eq. (12) within a factor of 1.1 (see Table 2 and SI-Excel-1).

$HOCl$ and $HFeO_4^-$. Even though HOCl and $HFeO_4^-$ show a considerable reactivity to aniline (i.e. $k > 10^2\,M^{-1}\,s^{-1}$), only a few rate constants are available for substituted anilines. One k_{ArNH2}-value is available for HOCl, which is the reaction with sulfamethoxazole ($k = 2.4 \times 10^3\,M^{-1}\,s^{-1}$, Dodd and Huang, 2004). For $HFeO_4^-$, k_{ArNH2}-values have been determined for the reaction with aniline and sulfonamide-antimicrobial compounds (sulfadimethoxine, sulfamethizole, sulfamethazine, sulfamethoxazole and sulfisoxazole) (Lee et al., 2009; Sharma et al., 2006). However, it was proposed that the determined k_{ArNH2}-values for the reaction of $HFeO_4^-$ might represent the k-value for the reaction of aniline-ferrate intermediates with aniline (Lee et al., 2009). More kinetic studies are needed to be able to develop reliable QSARs for the reactions of anilines, especially with HOCl, and $HFeO_4^-$.

3.1.3. Benzene derivatives

O_3 shows considerable reactivity, albeit with a wide range of reactivity towards several sub-classes of benzene derivatives (BZD) such as phenols, anilines, alkyl-/alkoxy-benzenes, and halo-benzenes etc ($0.1 < k < 10^{10}\,M^{-1}\,s^{-1}$). Currently, there are at least 67 k-values available for the reaction of O_3 with benzene derivatives, which may produce useful QSARs. Correlation analysis was performed based on benzene as a reference compound and using different types of the Hammett σ constants. In the case of mono- or di-substituted benzenes, multiple sites for O_3 attack are possible. Each scenario of O_3 attack results in a different value of $\sum(\sigma)$. To solve this problem, O_3 attack was assumed to occur at the site where the $\sum(\sigma)$ value is the lowest. This assumption is reasonable because more negative σ values indicate more electron density on the benzene, which would be more susceptible to electrophilic attack. Overall, a good correlation was found only when applying a few restrictions as follows: 1) $\sum \sigma_p^+$ had to be used as sole descriptor variable. This means that σ_p^+ was used instead of σ_o^+ and σ_m^+, and 2) the k-values for the reaction of O_3 with fourteen anilines and three other compounds such as 2,4-dichlorophenolate, nitrobenzene, and benzaldehyde were excluded as outliers in the QSAR. Fig. 7 shows the resulting linear correlation for the reaction of O_3 with benzene derivatives (BZD). The obtained Eq. (13) is shown Table 1 (see also SI-EXCEL-1).

The two restrictions applied for developing Eq. (13) can be acceptable when considering the diverse structures of the compounds and the corresponding different reaction mechanisms for their reaction with O_3. Here, our intention was to develop a useful semi-empirical correlation covering as many benzene derivatives as possible with minimal restrictions. Eq. (13) predicts 30 out of 50 (60%) k_{BZD}-values within a factor of
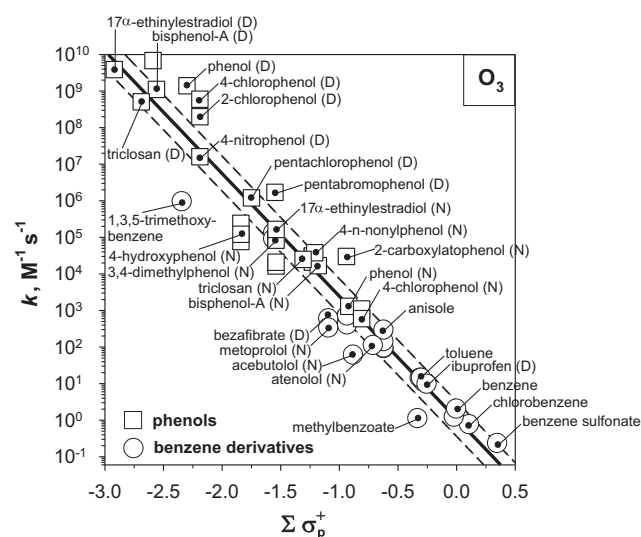
Fig. 7 – Correlation between the second-order rate constants (k) for the reactions of O_3 with benzene derivatives (e.g. phenols, alkylbenzenes etc) vs. $\sum \sigma_p^+$ (Eq. (13), Table 1) which are determined using benzene as a reference compound instead of phenol (see main text for further explanation). 'D' and 'N' in parenthesis indicate 'dissociated' and 'non-dissociated' species, respectively. Some symbols are not named due to space limitation: dissociated phenols such as 4-n-nonyl-phenolate; non-dissociated phenols such as 2-chloro-, 2-methyl-, 3-methyl-, 4-methyl-, 2,3-dimethyl-, 2,4-dimethyl-, 2,6-dimethyl-, 2-hydroxy- and 3-hydroxy-phenol, benzene derivatives such as 1,4-dimethoxy-, 3,4-dimethoxy-, ethyl-, isopropyl-, 1,2,3-trimethyl-, 1,3,5-trimethyl-benzene, and *ortho*-xylene, *meta*-xylene, *para*-xylene and benzoate (data, SI-EXCEL-1).
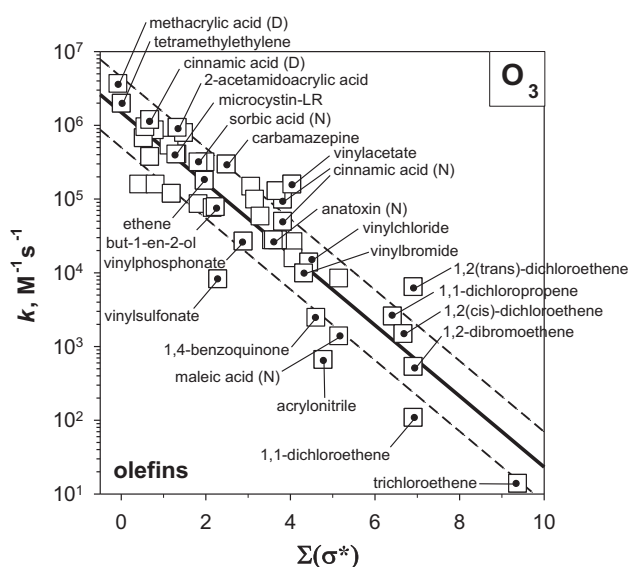

Fig. 8 – Correlation between the second-order rate constants (k) for the reactions of O_3 with olefins vs. $\sum \sigma^*$ (Eq. (14), Table 1). 'D' and 'N' in parenthesis indicate 'dissociated' and 'non-dissociated' species, respectively. Some symbols are not named due to space limitation: acrylamide, acrylic acid (D), acrylic acid (N), cephalexin (D), fumaric acid (N), *cis*-3-hexen-1-ol, methacrylic acid (N), β-ionone, 4-methoxy-cinnamic acid (D), *cis-cis*-muconic acid (N), *trans-trans*-muconic acid (N), 4-nitro-cinnamic acid (D), *trans-cis*-2,6-nonadienal, muconic acid (N), oseltamivir acid (D), 1-penten-3-one, propene, tylosin and vinylphosphonic acid (N) (data, SI-EXCEL-1).

1/3–3. Eq. (13) can be useful to predict the k-values for the reaction of O_3 with some benzene derivatives, such as alkyl-, alkoxy-, and halo-benzenes. For phenols, Eqs. (7) and (8) can be applied preferentially because they give better predictions than Eq. (13). Currently, the k_{BZD}-values of O_3 are known for several micropollutants. Eq. (13) predicts the k_{BZD}-values with difference of less than a factor of 3 for atenolol/non-dissociated and ibuprofen/dissociated. However, the predicted k_{BZD}-values for bezafibrate/dissociated, metoprolol/non-dissociated and acebutolol/non-dissociated differ from the measured ones by a factor of 7.1, 12.6 and 13.7, respectively (see Fig. 7 and SI-Excel-1).

3.1.4. Olefins
Among the selective oxidants, only O_3 and $HFeO_4^-$ show a reactivity towards olefins (e.g. $k > 10\ M^{-1}\ s^{-1}$) while ClO_2 and HOCl react very slowly with olefins (e.g. $k < 1\ M^{-1}\ s^{-1}$). For O_3, 74 rate constants are available while only two rate constants are known for $HFeO_4^-$. Therefore, the correlation analysis was performed only for O_3 (SI-Excel-1).

O_3 (Fig. 8). Correlations based on the Hammett σ constants turned out to be poor. Therefore, the Taft σ^* constants were selected. The k-values for the reaction of O_3 with nucleic acids and their constituents as olefin-containing compounds

(Theruvathu et al, 2001) were excluded in the QSAR analysis because their Taft σ^* constants were difficult to calculate (due to heterocyclic structure). 12 out of 74 k-values for the reaction of O_3 could not be used because Taft σ^* constants are not available for the substituents, such as, m-, p-dihydroxy-phenyl-, $-CH=CH-CO_2^-$, $-PO_3^{2-}$, $-PO(OH)_2$ etc (see SI-Excel-1). In addition, 13 out of 74 k-values were excluded as outliers because the predicted k_{olefin}-values differed significantly from the measured values by a factor of >50. These compounds typically contain carboxylate anion (e.g. maleic acid/dissociated) or cyclohexene with carbonyl (e.g. progesterone) as substituents (see SI-Excel-1). Finally, 48 k-values were used to develop Eq. (14) for the linear correlation of ozone for k_{olefin}. (Table 1 and Fig. 8).

O_3 shows a high reactivity towards olefins with electron-donating substituents (e.g. $k_{olefin} > 10^5\ M^{-1}\ s^{-1}$ for alkyl, alkoxy, and hydroxyl). However, with an increasing number of electron-withdrawing substituents such as halogens and carbonyls, the k_{olefin}-values decrease significantly with a ρ slope of −0.49. For example, the k_{olefin}-values of ozone with trichloroethene (TCE) and tetrachloroethene (PCE) are 140 and <0.1 $M^{-1}\ s^{-1}$, respectively. 33 out of 48 (69%) k_{olefin}-values were predicted by Eq. (14) within a factor of 1/3–3. In addition to those halogenated alkenes, the k_{olefin}-values with several olefin-containing micropollutants are available. The k_{olefin}-values for anatoxin-a/non-dissociated, cephalexin/dissociated, *cis*-3-hexen-1-ol, microcystin-LR, *trans-cis*-2,6-

nonadienal, oseltamivir acid/dissociated, 1-penten-3-one and tylosine were predicted with Eq. (14) within a factor of 1/3—3. However, the predicted k_{olefin}-value for carbamazepine and β-ionone differ from the measured values by a factor of 3.2 and 3.9, respectively (see SI-Excel-1).

$HFeO_4^-$. The k_{olefin}-values for $HFeO_4^-$ reactions are available only for butenol ($k_{olefin} = 19\,M^{-1}\,s^{-1}$) and carbamazepine ($k_{olefin} = 70$ or $110\,M^{-1}\,s^{-1}$) (Hu et al., 2009; Lee et al., 2009). Compared to the k-values for $HFeO_4^-$ reactions with phenolates and anilines (i.e. k_{PhO^-} and k_{ArNH2}), the k_{olefin}-values are about two or three orders of magnitude lower.

3.1.5. Amines

Alkylamines have three sub-classes depending on the number of alkyl carbons attached to the nitrogen, i.e. primary (1°, RNH_2), secondary (2°, R_2NH), and tertiary (3°, R_3N) amines. Ammonia, hydroxylamine and halo-amines as inorganic amines are sub-classes of amines. There are also halogenated-alkylamines and amide. In this study, the k-values of all these sub-classes of amines with structures such as $R_1-N(R_2)-R_3$ (R: alkyl, carbonyl, hydrogen, and hydroxyl) were considered in the QSAR analysis. All selective oxidants are in general reactive to alkylamines. Exceptions are found for the reaction of ClO_2 with 1° and 2° alkylamines and the reaction of $HFeO_4^-$ with 3° alkylamines, in which the k_{app}-values at near-neutral pH are typically $<10\,M^{-1}\,s^{-1}$. The selective oxidants are reactive to hydroxylamine but show much lower reactivity to ammonia, halo-amines, and amides. An exception for this is the fast reaction of HOCl with ammonia which forms chloramines ($HOCl + NH_3 \rightarrow NH_2Cl + H_2O$, $k = 3 \times 10^6\,M^{-1}\,s^{-1}$, Deborde and von Gunten, 2008).

Taft σ^* constants were used to develop QSARs for amines. Alkylamines typically have pK_a values in the range of 9—11. Since N-protonated alkylamine moieties are not susceptible to oxidation, the reactivity is determined by the concentration of N-deprotonated alkylamine species. Therefore, the corresponding rate constant, k_{amine}, are typically known for deprotonated alkylamine species. For O_3, ClO_2, and HOCl, a considerable number of k-values are available to develop QSARs. However, a limited number of k-values are available for the reaction of $HFeO_4^-$ with amines and thus reliable QSARs could not be obtained.

In the correlation analysis, all sub-classes of amines were considered together in the first step. When one class of amine showed significantly different k_{amine}-values from the rest of the corresponding amine-class was excluded in the next round. This process was repeated until the best correlations were obtained.

O_3 (Fig. 9). The linear correlation of ozone for k_{amine} is shown in Eq. (15) in Table 1. Eq. (15) includes the k_{amine}-values of not only 1°, 2°, and 3° alkylamines but also several inorganic amines such as hydroxylamine, chloramines and bromamines. O_3 shows a high reactivity to 2° and 3° alkylamines: the k_{amine}-values are $6 \times 10^5 - 2 \times 10^7\,M^{-1}\,s^{-1}$ (Fig. 9). Based on typical pK_a values of 2° ($pK_a \sim 10$) and 3° alkylamines (pK_a of ~9), the k_{app}-values at pH 7 are $60 - 2 \times 10^5\,M^{-1}\,s^{-1}$. The k_{app}-values will increase a factor of 10 per pH unit in the pH range 6—9. The k_{amine}-values for 1° alkylamines are $5 \times 10^4 - 2 \times 10^5\,M^{-1}\,s^{-1}$, which are about one or two orders of magnitude lower than those for 2° and 3° alkylamines (Fig. 9).
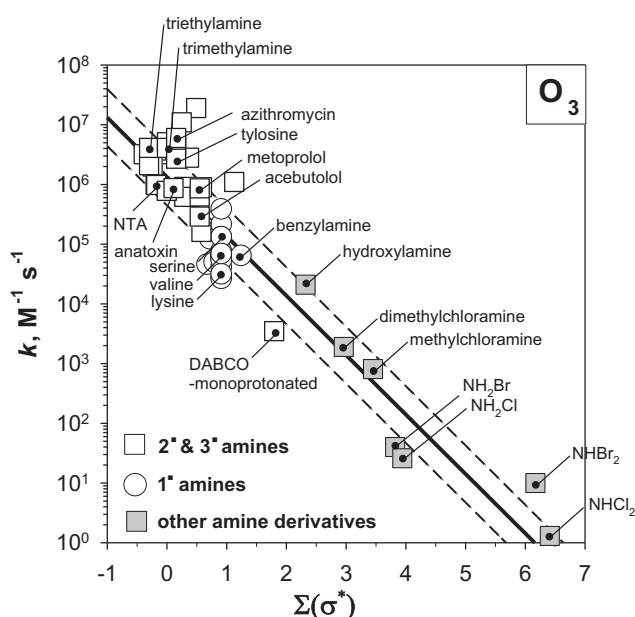

Fig. 9 – Correlation between the second-order rate constants (k) for the reactions of O_3 with amines & amine derivatives vs. $\sum\sigma^*$ (Eq. (15), Table 1). Some symbols are not named due to space limitation: 2° & 3° amines such as atenolol, ciprofloxacin, diethylamine, dimethylamine, N,N-dimethylcyclohexylamine, dimethylethanolamine, enrofloxacin, ethyl-N-piperazine carboxylate, EDTA, iminodiacetic acid, 1-methylpyrrolidine, roxithromycin and tramadol; 1° amines such as alanine, arginine, aspartate, n-butylamine, sec-butylamine, tert-butylamine, cyclohexanemethylamine, cyclohexylamine, glutamine, glycine, isoleucine, leucine and phenylalanine (data, SI-EXCEL-1).

The k_{app}-values at pH 7 for 1° alkylamines will then be $50 - 2 \times 10^2\,M^{-1}\,s^{-1}$ by assuming the pK_a of 10 for 1° alkylamines. Among inorganic amines, hydroxylamine shows a high reactivity to O_3: $k_{amine} = 2.1 \times 10^4\,M^{-1}\,s^{-1}$. However, haloamines such as NH_2Cl and $NHCl_2$, NH_2Br and $NHBr_2$ have a low reactivity to O_3 (i.e. $k < 40\,M^{-1}\,s^{-1}$). Ammonia, N,N-dimethylacetamide, N,N-dimethylformamide, and N,N-dimethylnitrosamine were not considered due to a much lower reactivity to O_3 than the predictions made by Eq. (15) (see SI-Excel-1).

Eq. (15) predicts 33 out of 54 (61%) k_{amine}-values within a factor of 1/3—3. The k_{amine}-values for the reaction of O_3 with several amine-containing micropollutants are available (Fig. 9). The k_{amine}-values for acebutolol, anatoxin-a (attack on the deprotonated amine, not on the double bond), atenolol, ciprofloxacin, DABCO, EDTA, EDTA-H⁺, enrofloxacin, metoprolol, NTA, tramadol and tylosine were predicted with a difference of less than a factor of 3. However, the predicted k_{amine}-values for azithromycin, DABCO-H⁺ and roxithromycin differ from the measured ones by a factor of 6.4, 6.2 and 4.8, respectively (see SI-Excel-1).

ClO_2 (Fig. 10). For ClO_2, two different correlations were established: one for the reaction with 3° alkylamines and the
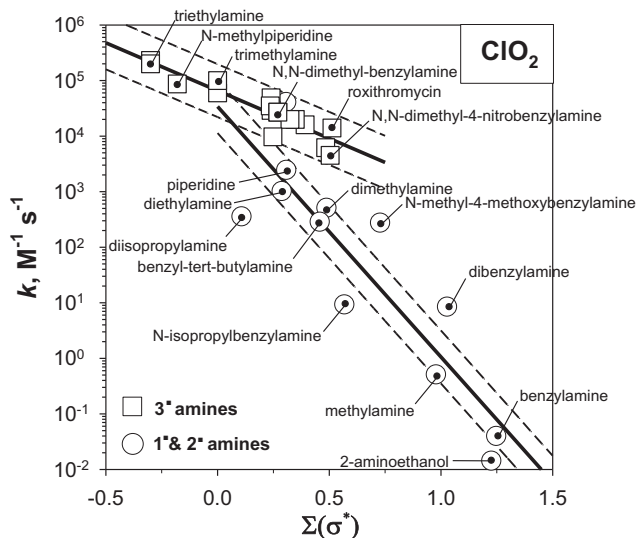
Fig. 10 — Correlation between the second-order rate constants (k) for the reactions of ClO_2 with 3° alkylamines (Eq. (16), Table 1) and with 1° & 2° alkylamines (Eq. (17), Table 1) vs. $\sum\sigma^*$. Some symbols are not named due to space limitation: 3° alkylamines such as N,N-dimethyl-3-chloro-, N,N-dimethyl-4-chloro-, N,N-dimethyl-4-fluoro-, N,N-dimethyl-3-methoxy-, N,N-dimethyl-4-methoxy-, N,N-dimethyl-4-methyl- and N,N-dimethyl-3-nitro-benzylamine, N,N-dimethyl-tert-butylamine and dimethylethanolamine (data, SI-EXCEL-1).
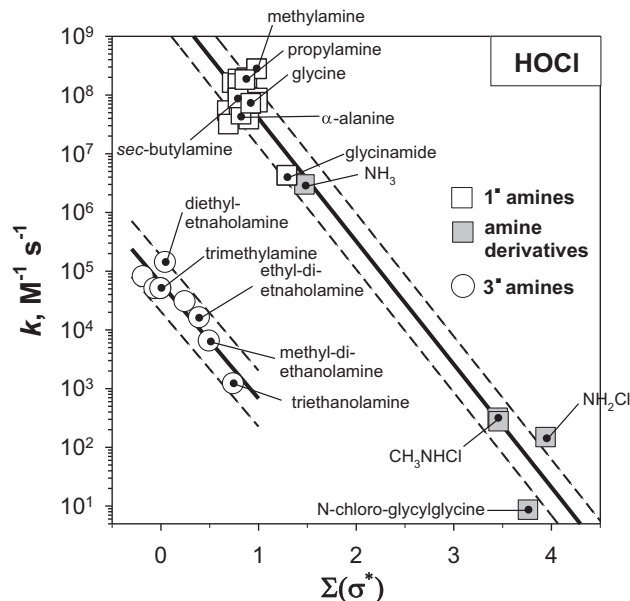

Fig. 11 — Correlation between the second-order rate constants (k) for the reactions of HOCl with 3° alkylamines (Eq. (18), Table 1) and with 1° alkylamines and amine derivatives (halo-amines and ammonia) vs. $\sum\sigma^*$ (Eq. (19), Table 1). Some symbols are not named due to space limitation: 3° alkylamines such as dimethylethanolamine, N,N-dimethylglycine and (N-methyl)-piperidine, 1° alkylamines such as β-alanine, 2-amino-, 3-amino- and 4-amino-butyric acid, 3-amino-iso-butyric acid, 2-amino-hexanoic acid, n-butylamine, iso-butylamine, tert-butylamine, ethylamine and iso-propylamine, amine derivatives such as N-chloro-β-alanine.

other with 1° & 2° alkylamines, which are shown in Eqs. 16 and 17 in Table 1, respectively. ClO_2 shows a high reactivity to 3° alkylamines: the $k_{3°amine}$ values are $5 \times 10^3 - 2 \times 10^5 \, M^{-1} s^{-1}$ (Fig. 10). Based on typical pK_a values of 3° alkylamines (pK_a ~9), the k_{app}-values at pH 7 for 3° alkylamines are $50 - 2 \times 10^3 \, M^{-1} s^{-1}$. In addition, the k_{app}-values will increase by a factor of 10 per pH unit in the pH range 6—9. In contrast, ClO_2 shows a relatively low reactivity to 1° and 2° alkylamines. In addition, $k_{1°\&2°amine}$-values are significantly influenced by the substituent effect with a ρ slope of −4.51. The k-values with 2° alkylamines, are $10 - 10^4 \, M^{-1} s^{-1}$. Considering a typical pK_a of 2° alkylamines (pK_a ~10), the k_{app}-values at pH 7 for 2° alkylamines are $10^{-2} - 10 \, M^{-1} s^{-1}$. The k-values with 1° alkylamines are even below $1 \, M^{-1} s^{-1}$. Therefore, most of 1° and 2° alkylamines react slowly with ClO_2 in the pH range 6—9 (e.g. k_{app}-values at pH $7 < 10 \, M^{-1} s^{-1}$). Eq. (16) predicts all 16 $k_{3°amine}$-values within a factor of 1/3—3. In contrast, Eq. (17) shows a poor correlation: only 6 out of 12 (50%) $k_{1°\&2°amine}$-values were predicted within a factor of 1/3—3.

HOCl (Fig. 11). For HOCl, two different correlations were established: one for the reaction with 3° alkylamines and the other with 1° alkylamines and amine derivatives (haloamines and ammonia), which are shown in Eqs. 18 and 19 in Table 1, respectively. In contrast to the case of O_3 and ClO_2, HOCl shows a lower reactivity to 3° alkylamines than 1° and 2° alkylamines (Fig. 11). Nevertheless, HOCl shows still a considerable reactivity to 3° alkylamines ($k_{3°amine} = 10^3 - 10^5 \, M^{-1} s^{-1}$). Therefore, the k_{app}-values at pH 7 for 3° alkylamines are $10 - 10^3 \, M^{-1} s^{-1}$ based on a typical pK_a value of 3° alkylamines (pK_a ~9). The

reactivity of HOCl toward 1° and 2° alkylamines is very high ($k_{1°amine}$ and $k_{2°amine} = 4 \times 10^6 - 3 \times 10^8 \, M^{-1} s^{-1}$). Based on typical pK_a of 1° and 2° alkylamines (pK_a ~10), the k_{app}-values at pH 7 for 1° and 2° alkylamines are $4 \times 10^3 - 3 \times 10^5 \, M^{-1} s^{-1}$. Poor correlations were found ($r^2 = 0.03$) when considering the k_{amine}-values of 1° and 2° alkylamines together or 2° alkylamine only. Therefore, 2° amines were not considered for our correlations. Instead, a good correlation (i.e. Eq. (19)) was found when considering the k_{amine}-values of 1° alkylamines together with those of halo-amines and ammonia (Fig. 11).

Eq. (18) predicts all eight $k_{3°amine}$-values within a factor of 1/3—3. The $k_{3°amine}$-value for the reaction with enrofloxacin as 3° alkylamine-containing micropollutant has been determined to be $1.6 \times 10^3 \, M^{-1} s^{-1}$ (Dodd et al., 2005), which differs from the predicted value by a factor of 40 (see SI-Excel-1). Therefore, it was not included in developing Eq. (18) (see SI-Excel-1). Eq. (19) predicts 17 out of 22 (77%) $k_{1°amine}$-values within a factor of 1/3—3. Even though good correlations were not found for 2° alkylamines, their k-value are typically in the range of $10^7 - 10^8 \, M^{-1} s^{-1}$ (see SI-Excel-1). In accordance with this, the k-value for the reaction with ciprofloxacin, a 2° alkylamine-containing micropollutant is $4.9 \times 10^7 \, M^{-1} s^{-1}$ (Dodd et al., 2005).

$HFeO_4^-$. The number of determined rate constants for the reaction of $HFeO_4^-$ with amines is limited. Less than 10 k-

values are currently known for some alkylamines and inorganic amine species (Lee et al., 2008, 2009; Noorhasan et al., 2010; Zimmermann et al., 2012). No clear correlations were found among these k-values. Some simple calculations were performed to give rough estimates of k-values for the reaction of $HFeO_4^-$ with amines. The k-values for the reaction with 3° alkylamines are 2×10^2–$1 \times 10^3 \, M^{-1} \, s^{-1}$. With typical pK_a values of 3° alkylamines ($pK_a \sim 9$), the k_{app}-values at pH 7 for 3° alkylamines are estimated to be 2–10 $M^{-1} \, s^{-1}$. The k-values for the reaction with 2° alkylamines are 4.4×10^3 and $1.8 \times 10^4 \, M^{-1} \, s^{-1}$ for ciprofloxacin and dimethylamine, respectively, which are about one order of magnitude higher than those for 3° alkylamines. With typical pK_a values of 2° amines ($pK_a \sim 10$), the k_{app}-values at pH 7 for 2° amines are estimated to be 4.4–18 $M^{-1} \, s^{-1}$. However, the k_{app}-values at pH 7 for ciprofloxacin and enrofloxacin are rather high due to the low pK_a values of these two cyclic amine moieties ($pK_a = 7.7$ and 8.8, respectively). Finally, the k-value for the reaction with 1° alkylamines (i.e. glycine) was determined as $3.0 \times 10^4 \, M^{-1} \, s^{-1}$ (Noorhasan et al., 2010).

3.1.6. Cross-correlations

Rate constants for the reactions of oxidants can be used as descriptor variables in correlation analysis (Canonica and Tratnyek, 2003; Deborde and von Gunten, 2008). Fig. 12 shows two developed correlations between the logarithm of k-values for the reaction of O_3 vs. ClO_2 (Fig. 12a) and O_3 vs. HOCl (Fig. 12b) with various aromatic compounds. The aromatic compounds include mostly phenols (dissociated and non-dissociated) but also some anilines (aniline, diclofenac, and sulfamethoxazole), alkoxybenzene (anisole), polycyclic-aromatic (pyrene), and pyrimidine derivative (trimethoprim). Eqs. (20) and (21) are the resulting correlations for the reaction of O_3 vs. ClO_2 and O_3 vs. HOCl, respectively.

11 out of 16 (69%) k-values were predicted by Eq. (20) within a factor of 1/3–3. 13 out of 24 (54%) k-values were predicted by Eq. (21) within a factor of 1/3–3. For diclofenac and sulfamethoxazole, the k-values for the reaction with both O_3 and ClO_2 are known, therefore Eq. (20) could be tested to predict these

k-values. The result shows that Eq. (20) predicts these two k-values with differences of less than a factor of 3 (Fig. 12a). In the case of Eq. (21), the k-values for the reaction of O_3 and HOCl were correlated with differences of less than a factor of 3 for the following four micropollutants: steroid estrogens (17α-ethinylestradiol, 17β-estradiol, estrone, and estriol/dissociated bisphenol-A/dissociated, steroid estrogens/non-dissociated, and 4-n-nonylphenol/non-dissociated. However, for the other micropollutants, Eq. (21) predicts the k-values poorly: the predicted k-values differ from the measured ones by a factor of 4.7 for 4-n-nonylphenol/dissociated, 4.4 for triclosan/dissociated, 44 for sulfamethoxazole, 7.6 for trimethoprim/fully dissociated, and 3.3 for bisphenol-A/non-dissociated (Fig. 12b). Eqs. (20) and (21) can be useful for predicting k-values of aromatic compounds when the k-value of at least one oxidant is known. However, because the correlations are derived mainly based on phenols, they should be cautiously applied to other non-phenolic aromatic compounds, such as anilines and polycyclic aromatic compounds.

3.2. Estimation methods of k-values for HO• reactions

This section will briefly introduce some principles and estimation methods for HO• reaction rate constants. HO• react with organic compounds primarily in four ways: (1) by addition to an olefin or an aromatic system, (2) by abstraction of a hydrogen atom from a carbon atom, (3) electron transfer reactions and (4) by reaction with sulfur-, nitrogen-, or phosphorus-moieties (Buxton et al., 1988; Minakata et al., 2009; Schwarzenbach et al., 2003). Currently, there are a few thousands k-values available for the reaction of HO• with organic compounds. These $k_{HO•}$-values show that nearly diffusion-controlled values (i.e. $k_{HO•} = 3 \times 10^9$–$10^{10} \, M^{-1} \, s^{-1}$) are observed for compounds containing 1) aromatic rings or olefins with electron-donating or even weakly-electron-withdrawing substituents, 2) aliphatic groups with multiple H-atoms which can be easily abstracted, and 3) organic sulfur- or amine-moieties (Buxton et al., 1988). Many of the emerging organic micropollutants fulfill the above-described criteria, and
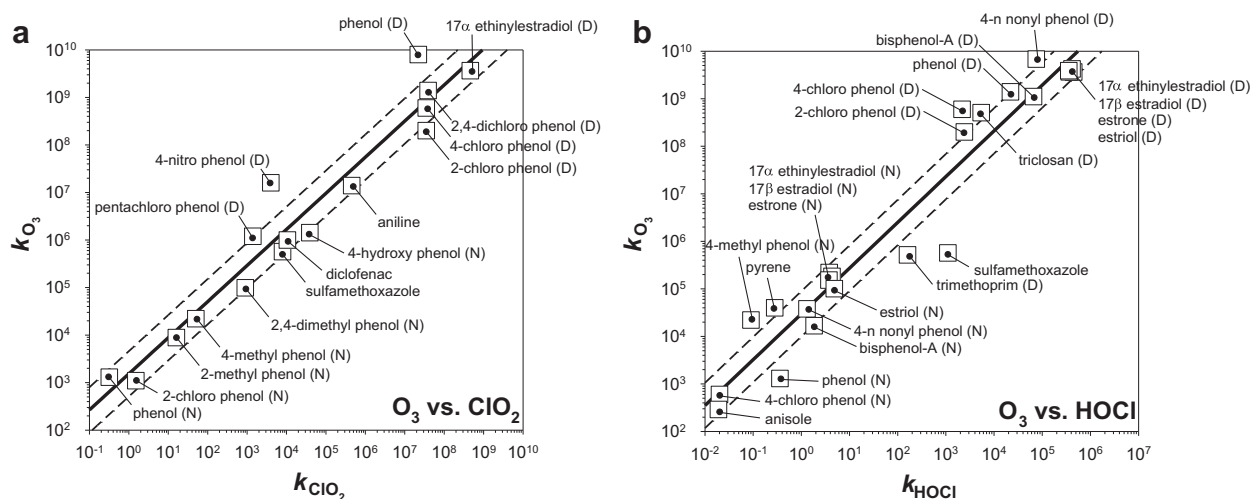
Fig. 12 – Linear cross correlations for selected aromatic compounds (mostly phenols) between (a) log $k_{aromatic}$ (O_3) and log $k_{aromatic}$ (ClO_2) (Eq. (20), Table 1) and (b) log $k_{aromatic}$ (O_3) and log $k_{aromatic}$ (HOCl) (Eq. (21), Table 1). 'D' and 'N' in parenthesis indicate 'dissociated' and 'non-dissociated' species, respectively (data, SI-EXCEL-1).

consistent with this fact, the $k_{HO^•}$-values for most emerging micropollutants have been known to be $\geq 3 \times 10^9 \, M^{-1} \, s^{-1}$ (see Table 2 for examples). Organic micropollutants that show a low reactivity to $HO^•$ (i.e. $k_{HO^•} < 3 \times 10^9 \, M^{-1} \, s^{-1}$) are typically small sized (e.g. $MW < 200 \, Da$) and contain electron-withdrawing substituents in their saturated carbon skeletons. These include methyl tert-butyl ether (MTBE, $k_{HO^•} = 1.9 \times 10^9 \, M^{-1} \, s^{-1}$), chloroform ($k_{HO^•} = 5 \times 10^7 \, M^{-1} \, s^{-1}$), and N-nitrosodimethyl-amine (NDMA, $k_{HO^•} = 4.5 \times 10^8 \, M^{-1} \, s^{-1}$) (Buxton et al., 1988, Lee et al., 2007). Therefore, as a rule of thumb, most emerging organic micropollutants with molecular sizes larger than 200 Da containing ERMs, will show $k_{HO^•}$-values in the range of $3 \times 10^9 – 10^{10} \, M^{-1} \, s^{-1}$, varying by a factor of ~ 3.

In addition to the aforementioned simple estimation method for $HO^•$ rate constants, there have been a few more sophisticated estimation methods for $HO^•$ rate constants. One of these methods is based on the group contribution method (GCM) which has been traditionally developed for predicting gas-phase $HO^•$ reaction rate constants (Minakata et al., 2009; Schwarzenbach et al., 2003). In the GCM method, the $HO^•$ reaction rate constant is determined by the reaction mechanism and effect of the neighboring functional group. As the reaction mechanism, it considers: (1) H-atom abstraction from C–H; (2) $HO^•$ addition to olefins; (3) $HO^•$ addition to aromatic rings; and (4) reaction with N-, P-, and S-containing moieties. For each of these reaction mechanisms, there are 'group rate constants' which represent the reactivity of a reference reaction and 'group contribution factors' which represent the effect of neighboring functional groups on the reactivity of a reference reaction. Minakata et al (2009) reported 66 group rate constants and 80 substituent factors for these four reaction mechanisms, which were determined based on 310 $k_{HO^•}$-values (Minakata et al., 2009). For H-abstraction as an example, there exist three group rate constants with primary- (CH_3R_1, $k_{prim} = 1.18 \times 10^8 \, M^{-1} \, s^{-1}$), secondary- ($CH_2R_1R_2$, $k_{sec} = 5.11 \times 10^8 \, M^{-1} \, s^{-1}$) and tertiary- C-H bonds ($CHR_1R_2R_3$, $k_{tert} = 19.9 \times 10^8 \, M^{-1} \, s^{-1}$). The overall H-atom abstraction rate constant, $k_{HO^•}$ (H-abstr) can then be obtained from the sum of these partial rate constants (Eq. (22)):

$$k_{HO^•} \, (H - abstr) = 3 \sum k_{prim} X_{R1} + 2 \sum k_{sec} X_{R1} X_{R2} + \sum k_{tert} X_{R1} X_{R2} X_{R3} \tag{22}$$

where X_{R1}, X_{R2}, and X_{R3} are the group contribution factors for R_1, R_2 and R_3 substituents, respectively. Finally, the total rate constant, $k_{HO^•}$ (total), can be expressed by the sum of four rate constants as shown in Eq. (23):

$$k_{HO^•} \, (total) = k_{HO^•} \, (H - abstr) + k_{HO^•} \, (olefin) + k_{HO^•} \, (Ar) + k_{HO^•} \, (NPS) \tag{23}$$

where $k_{HO^•}$ (H-abstr), $k_{HO^•}$ (olefin), $k_{HO^•}$ (Ar), and $k_{HO^•}$ (NPS) are the rate constants for the aforementioned mechanisms, 1–4, respectively.

3.3. Prediction of k-values for the reaction of selective oxidants and HO$^•$ with micropollutants

As a demonstration, the QSARs from this study were used to predict k-values for the reaction of the selective oxidants with

overall 16 selected micropollutants. In the case of $HO^•$, the group contribution method developed by Minakata et al (2009) was used to estimate the k-values. The selected micropollutants include five phenolic- (acetaminophen, bisphenol-A, 17α-ethinylestradiol, 4-n-nonylphenol, and triclosan), two aniline- (sulfamethoxazole and diclofenac), three olefin- (anatoxin/non-dissociated, carbamazepine, and microcystin-LR), and four amine-containing compounds (anatoxin/disso-ciated, ciprofloxacin, enrofloxacin, and roxithromycin). In addition, gemfibrozil and naproxen were included as substituted benzenes. Therefore, the selected micropollutants cover a range of ERMs which are the site of attack by oxidants. These micropollutants were also chosen based on their environmental relevance. They are mostly pharmaceuticals and hormones which are discharged from municipal wastewater effluents. In addition, anatoxin and microcystin-LR may be produced during algal blooms.

Table 2 summarizes the predicted k-values and compares them with the measured ones if data are available. For the selective oxidants, 39 out of the 45 (87%) predicted k-values were within a factor of 1/3–3. The prediction of k-values was also applied to other emerging micropollutants which are not listed in Table 2 (see SI-Excel-1). Overall, 75 out of the 97 (77%) predicted k-values were within a factor of 1/3–3. It should be noted that since all measured k-values were already included in developing QSARs for the selective oxidants, the comparison between the measured and predicted values just confirms again the goodness of the calibration. For $HO^•$, the GCM method predicts the k-values within a factor of 1/2–2. One exception was the reaction of $HO^•$ with anatoxin-a. Its k-value was predicted to be $\sim 10^{10} \, M^{-1} \, s^{-1}$, which is 3.3 times higher than the measured value ($k = 3 \times 10^9 \, M^{-1} \, s^{-1}$, Onstad et al., 2007). Finally, 29 new k-values were predicted for the reaction of selective oxidants and $HO^•$ (Table 2), which will be useful in estimating the elimination of these micropollutants during oxidative water treatment.

3.4. Uncertainty in predicting micropollutant elimination by QSARs

In this study, 18 QSARs were developed based on 412 k-values for the reaction of the selective oxidants with (mostly) organic compounds containing various ERMs. 217 and 303 out of 412 (53 and 74%) k-values were predicted within a factor of 1/2–2 and 1/3–3, respectively (see SI-Excel-1). In addition, the GCM method for $HO^•$ reaction showed a prediction of k-values within 1/2–2 (Minakata et al., 2009; see also Table 2). Therefore, as a rule of thumb, the k-values predicted by these QSARs have a potential error of a factor of up to 9, which is also commonly found in experimentally determined k-values.

Since we are interested in using k_{app}-values to predict micropollutant elimination during oxidative water treatment, it is of interest to know how the uncertainty in the calculated k-values affects the prediction of elimination rates. For this, Eq. (3) was used to calculate the uncertainty propagation from 'k_{app}-value' to 'elimination'. In the first step, the % elimination of micropollutant, P (i.e. $(1 - [P]/[P]_0) \times 100$) was calculated as a function of oxidant exposure by using a certain k_{app}-value. In the next step, the % P elimination was calculated using the same oxidant exposure but with k_{app}-values that were three-

fold larger or smaller than before (i.e. $3k_{app}$- or $1/3k_{app}$-values). Fig. 13a shows the calculated results. The uncertainty in the predicted % P elimination can be defined as the difference of $(1 - [P]/[P]_0) \times 100$ values obtained using $3k_{app}$- and $1/3k_{app}$-values. For example, the length of arrows in Fig. 13a represents the uncertainty at various levels of % P elimination. Fig. 13b shows the uncertainty in the predicted % P elimination as a function of the % P elimination levels. When the % P elimination is less than 10% or higher than 99%, the uncertainty is lower than 24%. In other words, even when the predicted k_{app}-value has uncertainty of a factor of 9, micropollutant eliminations can be still predicted with less than 24% error. However, when the % P elimination is in between 10% and 99%, the uncertainty can be higher than 24%. The largest uncertainty (i.e. 68%) is observed when the % P elimination is 57% (Fig. 13b).

Based on the above exercise, the QSARs developed for the selective oxidants are good enough to estimate micropollutant elimination, especially for the cases of high or low micropollutant eliminations. This means that when predicting high or low k_{app}-values, there is potentially low uncertainty (e.g. <24%) in the predicted levels of micropollutant elimination. The ex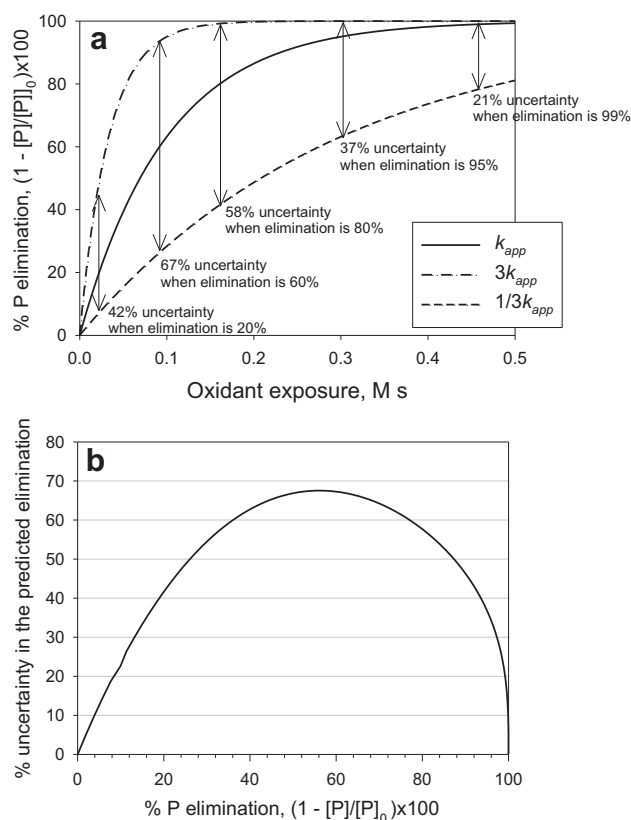act magnitude of k_{app}-values in this criterion depends on the type of the selective oxidant and application. During ozonation of secondary wastewater effluents for example, micropollutants having k_{app}-values for the reaction with O_3 higher than $10^4\, M^{-1}\,s^{-1}$ are eliminated typically > 99% at O_3 dose/DOC of higher than 0.6 (mass ratio) (Lee and von Gunten, 2010; Zimmermann et al., 2011). In addition, micropollutants having k_{app}-values less than $10\, M^{-1}\,s^{-1}$ are eliminated <10% by O_3 alone for the same experimental conditions (without considering the oxidation by $HO^\bullet$). Therefore, for these high or low k_{app}-values, a factor of 9 uncertainty in the predicted k_{app}-values results in less than 24% uncertainty in predicted eliminations. However, for the intermediate k_{app}-values, the predicted eliminations will have potential uncertainty of up to 68%.

In the case of $HO^\bullet$, the situation is different from the selective oxidants. In UV/H_2O_2 treatment of secondary wastewater effluent for example, eliminations of most micropollutants remain 10–90% at typical treatment conditions (e.g. UV dose = 300–700 mJ cm^{-2} and H_2O_2 = 10–20 mg L^{-1}) (Lee and von Gunten, 2010; Rosario-Ortiz et al., 2010). This relatively low elimination efficiency of micropollutants during treatment by $HO^\bullet$ is due to the significant scavenging of $HO^\bullet$ by water matrices (e.g. dissolved organic matter and carbonate) (Lee and von Gunten, 2010). Therefore, uncertainty in predicted micropollutant elimination can be high by uncertainty in k-values based on the discussion above. However, the uncertainty in k-values estimated by the GCM method (a factor of 4) is smaller than those by the QSARs for selective oxidants (a factor of 9).

4. Conclusions

- 18 QSARs were developed for the reaction of selective oxidants (O_3, ClO_2, $HOCl$, and $HFeO_4^-$) with organic compounds containing various ERMs. 6 QSARs could be established for the reaction of O_3 with phenols, phenolates, anilines, benzene derivatives, olefins, and amines based on 203 k-values. 5 QSARs could be established for the reaction of ClO_2 with phenols, phenolates, anilines, 3° amines and 1° & 2° amines based on 79 k-values. 3 QSARs could be established for the reaction of $HOCl$ with phenolates, 3° amines and 1° amines based on 65 k-values. 2 QSARs could be established for the reaction of $HFeO_4^-$ with phenols and phenolates based on 25 k-values. In addition, 2 cross-correlations were established between the logarithm k-values for the reaction of O_3 vs. ClO_2 and O_3 vs. $HOCl$ with aromatic compounds based on 40 k-values. 303 out of 412 (74%) k-values were predicted by the developed QSARs within a factor of 1/3–3 compared to the measured values. This level of uncertainty in k-values obtained from the QSAR predictions is comparable to the uncertainty in experimentally determined k-values.

- The established QSARs can be used to predict the k-values for emerging micropollutants and assess their transformation potential during oxidative water treatment. This could be demonstrated for 16 selected micropollutants that contain ERMs and have environmental relevance: 39 out of the 45 (87%) predicted k-values were found to be within a factor 1/3–3 compared to the measured values.

Fig. 13 – (a) Predicted % elimination of micropollutant as a function of oxidant exposure using three different k_{app}-values such as k_{app}, $3k_{app}$ and $1/3k_{app}$ ($k_{app} = 10\, M^{-1}\,s^{-1}$ was applied for calculations), the arrows represent the % uncertainty in the predicted P elimination (i.e. {% elimination at $3k_{app}$} − {% elimination at $1/3k_{app}$}) and (b) % uncertainty in the predicted P elimination as a function of % P elimination.

- Uncertainty in the predicted k-values by the QSARs can cause uncertainty in the prediction of micropollutant elimination during oxidative water treatment. At a factor of 9 variance in the predicted k-values, the predicted micropollutant elimination will have less than 24% uncertainty when the % micropollutant elimination is high (i.e. >99%) or low (i.e. <10%). However, when the elimination is in intermediate range (i.e. 10—90%), the uncertainty in predicted micropollutant elimination can increase up to 68%.

Acknowledgements

Appendix A. Supplementary material

Supplementary material associated with this article can be found, in the online version, at http://dx.doi.org/10.1016/j.watres.2012.06.006

REFERENCES

Albert, A., Serjeant, E.P., 1984. The Determination of Ionization Constants: A Laboratory Manual, third ed. Chapman & Hall, New York.

Asano, T., Burton, F.L., Leverenz, H.L., Tsuchihashi, R., Tchobanoglous, G., 2007. Water Reuse: Issues, Technologies, and Applications, first ed. McGraw-Hill, New York.

Black & Veatch Corporation, 2010. White's Handbook of Chlorination and Alternative Disinfectants, fifth ed. John Wiley & Sons, Inc, Hoboken, New Jersey.

Buxton, G.V., Greenstock, C.L., Helman, W.P., Ross, W.P., 1988. Critical review of rate constants for reactions of hydrated electrons, hydrogen atoms and hydroxyl radicals ($\cdot$OH/$\cdot$O$^-$) in aqueous solution. J. Phys. Chem. Ref. Data 17, 513—886.

Canonica, S., Tratnyek, P.G., 2003. Quantitative structure-activity relationships for oxidation reactions of organic chemicals in water. Environ. Toxicol. Chem. 22, 1743—1754.

Deborde, M., von Gunten, U., 2008. Reactions of chlorine with inorganic and organic compounds during water treatment-kinetics and mechanisms: a critical review. Water Res. 42, 13—51.

Deborde, M., Rabouan, S., Duguet, J.P., Legube, B., 2005. Kinetics of aqueous ozone-induced oxidation of some endocrine disruptors. Environ. Sci. Technol 39, 6086—6092.

Dodd, M.C., Huang, C.H., 2004. Transformation of the antibacterial agent sulfamethoxazole in reactions with chlorine: kinetics, mechanisms, and pathways. Environ. Sci. Technol 38, 5607—5615.

Dodd, M.C., Shah, A.D., von Gunten, U., Huang, C.-H., 2005. Interactions of fluoroquinolone antibacterial agents with aqueous chlorine: reaction kinetics, mechanisms, and transformation pathways. Environ. Sci. Technol 39, 7065—7076.

Dodd, M.C., Buffle, M.O., von Gunten, U., 2006. Oxidation of antibacterial molecules by aqueous ozone: moiety-specific reaction kinetics and application to ozone-based wastewater treatment. Environ. Sci. Technol 40, 1969—1977.

Dowideit, P., von Sonntag, C., 1998. Reaction of ozone with ethene and its methyl- and chlorine-substituted derivatives in aqueous solution. Environ. Sci. Technol 32, 1112—1119.

Gallard, H., von Gunten, U., 2002. Chlorination of phenols: kinetics and formation of chloroform. Environ. Sci. Technol 36, 884—890.

Gerrity, D., Gamage, S., Holady, J.C., Mawhinney, D.B., Quinones, O., Trenholm, R.A., Snyder, S.A., 2011. Pilot-scale evaluation of ozone and biological activated carbon for trace organic contaminants mitigation and disinfection. Water Res. 45, 2155—2165.

Hansch, C., Leo, A., Taft, R.W., 1991. A survey of Hammett substituent constants and resonance and field parameters. Chem. Rev. 91, 165—195.

Hansch, C., Leo, A., Hoekman, D., 1995. Exploring QSAR. Hydrophobic, Electronic, and Steric Constants. American Chemical Society, Washington, DC.

Hoigné, J., Bader, H., 1983a. Rate constants of reactions of ozone with organic and inorganic compounds in water-I. Non-dissociating organic compounds. Water Res. 17, 173—183.

Hoigné, J., Bader, H., 1983b. Rate constants of reactions of ozone with organic and inorganic compounds in water-II. Dissociating organic compounds. Water Res. 17, 185—194.

Hoigné, J., Bader, H., 1994. Kinetics of reactions of chlorine dioxide (OClO) in water-I. Rate constants for inorganic and organic compounds. Water Res. 28, 45—55.

Hollender, J., Zimmermann, S.G., Koepke, S., Krauss, M., McArdell, C.S., Ort, C., Singer, H., von Gunten, U., Siegrist, H., 2009. Elimination of organic micropollutants in a municipal wastewater treatment plant upgraded with a full-scale post-ozonation followed by sand filtration. Environ. Sci. Technol 43, 7862—7869.

Hu, L., Martin, H.M., Arce-Bulted, O., Sugihara, M.N., Keating, K.A., Strathmann, T.J., 2009. Oxidation of carbamazepine by Mn(VII) and Fe(VI): reaction kinetics and mechanism. Environ. Sci. Technol 43, 509—515.

Huber, M.M., Korhonen, S., Ternes, T.A., von Gunten, U., 2005. Oxidation of pharmaceuticals during water treatment with chlorine dioxide. Water Res. 39, 3607—3617.

Jonsson, M., Lind, J., Eriksen, T.E., Merenyi, G., 1993. O-H bond strengths and one-electron reduction potentials of multi-substituted phenols and phenoxy radicals—predictions using free-energy relationships. J. Chem. Soc., Perkin Trans. 2, 1567—1568.

Lee, Y., von Gunten, U., 2009. Transformation of 17α-ethinylestradiol during water chlorination: effects of bromide on kinetics, products, and transformation pathways. Environ. Sci. Technol 43, 480—487.

Lee, Y., von Gunten, U., 2010. Oxidative transformation of micropollutants during municipal wastewater treatment: comparison of kinetic aspects of selective (chlorine, chlorine dioxide, ferrate[VI], and ozone) and non-selective oxidants (hydroxyl radical). Water Res. 44, 555—566.

Lee, Y., Yoon, J., von Gunten, U., 2005. Kinetics of the oxidation of phenols and phenolic endocrine disruptors during water treatment with ferrate (Fe(VI)). Environ. Sci. Technol 39, 8978—8984.

Lee, C., Yoon, J., von Gunten, U., 2007. Oxidative degradation of N-nitrosodimethylamine by conventional ozonation and the advanced oxidation process ozone/hydrogen peroxide. Water Res. 41, 581—590.

Lee, C., Lee, Y., Schmidt, C., Yoon, J., von Gunten, U., 2008. Oxidation of suspected N-nitrosodimethylamine (NDMA) precursors by ferrate(VI): kinetics and effect on the NDMA

formation potential of natural waters. Water Res. 42, 433—441.

Lee, Y., Zimmermann, S.G., Kieu, A.T., von Gunten, U., 2009. Ferrate (Fe(VI)) application for municipal wastewater treatment: a novel process for simultaneous micropollutant oxidation and phosphate removal. Environ. Sci. Technol 43, 3831—3838.

Minakata, D., Li, K., Westerhoff, P., Crittenden, J., 2009. Development of a group contribution method to predict aqueous phase hydroxyl radical (HO•) reaction rate constants. Environ. Sci. Technol 43, 6220—6227.

Neta, P., Huie, E., Ross, A.B., 1988. Rate constants for reactions of inorganic radicals in aqueous solution. J. Phys. Chem. Ref. Data 17, 1027—1264.

Noorhasan, N., Patel, B., Sharma, V.K., 2010. Ferrate(VI) oxidation of glycine and glycylglycine: kinetics and products. Water Res. 44, 927—935.

Onstad, G.D., Strauch, S., Meriluoto, J., Codd, G.A., von Gunten, U., 2007. Selective oxidation of key functional groups in cyanotoxins during drinking water ozonation. Environ. Sci. Technol 41, 4397—4404.

Perrin, D.D., Dempsey, B., Serjeant, E.P., 1981. pK_a Prediction for Organic Acids and Bases. Champman and Hall, New York.

Pierpoint, A.C., Hapeman, C.J., Torrents, A., 2001. Linear free energy study of ring-substituted aniline ozonation for developing treatment of aniline-based pesticide wastes. J. Agri. Food Chem. 49, 3827—3832.

Pinkston, K.E., Sedlak, D.L., 2004. Transformation of aromatic ether- and amine-containing pharmaceuticals during chlorine disinfection. Environ. Sci. Technol 38, 4019—4025.

Rebenne, L.M., Gonzalez, A.C., Olson, T.M., 1996. Aqueous chlorination kinetics and mechanism of substituted dihydroxybenzenes. Environ. Sci. Technol 30, 2235—2242.

Reungoat, J., Macova, M., Escher, B.I., Carswell, S., Mueller, J.F., Keller, J., 2010. Removal of micropollutants and reduction of biological activity in a full scale reclamation plant using ozonation and activated carbon filtration. Water Res. 44, 625—637.

Rosario-Ortiz, F.L., Wert, E.C., Snyder, S.A., 2010. Evaluation of UV/H_2O_2 treatment for the oxidation of pharmaceuticals in wastewater. Water Res. 44, 1440—1448.

Schwarzenbach, R.P., Gschwend, P.M., Imboden, D.M., 2003. Environmental Organic Chemistry, second ed. John Wiley & Sons, Inc., New Jersey.

Schwarzenbach, R.P., Escher, B.I., Fenner, K., Hofstetter, T.B., Johnson, C.A., von Gunten, U., Wehrli, B., 2006. The challenge of micropollutants in aquatic systems. Science 313, 1072—1077.

Schwarzenbach, R.P., Thomas, E., Hofstetter, T.B., von Gunten, U., Wehrli, B., 2010. Global water pollution and human health. Annual Review of Environment and Resources 35, 109—136.

Sharma, V.K., Burnett, C.R., Millero, F.J., 2001. Dissociation constants of the monoprotic ferrate(VI) ion in NaCl media. Phys. Chem. Chem. Phys. 3, 2059—2062.

Sharma, V.K., Mishra, S.K., Nesnas, N., 2006. Oxidation of sulfonamide antimicrobials by ferrate(VI) [$Fe^{VI}O_4^{2-}$]. Environ. Sci. Technol 40, 7222—7227.

Snyder, S.A., Wert, E.C., Rexing, D.J., Zegers, R.E., Drury, D.D., 2006. Ozone oxidation of endocrine disruptors and pharmaceuticals in surface water and wastewater. Ozone Sci. Eng 28, 445—460.

Suarez, S., Dodd, M.C., Omil, F., von Gunten, U., 2007. Kinetics of triclosan oxidation by aqueous ozone and consequent loss of antibacterial activity: relevance to municipal wastewater ozonation. Water Res. 41, 2481—2490.

Ternes, T.A., Joss, A., 2006. Human Pharmaceuticals, Hormones and Fragrances. The Challenge of Micropollutants in Urban Water Management. IWA Publishing, London, New York.

Theruvathu, J.A., Flyunt, R., Aravindakumar, C.T., von Sonntag, C., 2001. Rate constants of ozone reactions with DNA, its constituents and related compounds. J. Chem. Soc., Perkin Trans. 2, 269—274.

Tratnyek, P.G., Hoigne, J., 1994. Kinetics of reactions of chlorine dioxide (OClO) in water-II. Quantitative structure-activity relationships for phenolic compounds. Water Res. 28, 57—66.

von Gunten, U., 2003. Ozonation of drinking water: Part I. Oxidation kinetics and product formation. Water Res. 37, 1443—1467.

Zimmermann, S.G., Schmukat, A., Schulz, M., Benner, J., von Gunten, U., Ternes, T.A., 2012. Kinetic and mechanistic investigations of the oxidation of tramadol by ferrate and ozone. Environ. Sci. Technol 46, 876—884.

Zimmermann, S.G., Wittenwiler, M., Hollender, J., Krauss, M., Ort, C., Siegrist, H., von Gunten, U., 2011. Kinetic assessment and modeling of an ozonation step for full-scale municipal wastewater treatment: micropollutant oxidation, by-product formation and disinfection. Water Res. 45, 605—617.